*Eurasian Journal of Science Engineering and Technology*

***Research Article***

# MODELING THERMAL BEHAVIOR IN HIGH-POWER SEMICONDUCTOR DEVICES USING THE MODIFIED OHM'S LAW

**Alex Mwololo KIMUYA[1,*]**

[1]*Department of Physical Science (Physics), Meru University of Science and Technology, Kenya*
*Phone: +254704600418*

## ABSTRACT

This paper addresses the challenge of thermal management in high-power semiconductor devices, where increasing power densities and complex operating environments demand more accurate thermal prediction methods. Traditional approaches often rely on simplified models that do not account for the crucial factor of temperature-dependent resistance variations. This limitation leads to inaccurate device temperature predictions, potentially compromising device reliability. This work proposes a novel approach for thermal management by introducing the first empirical application of a Modified Ohm's Law. This modified law incorporates an exponential term to account for the non-linear relationship between temperature, current, and resistance. The paper demonstrates through simulations and empirical validation that the Modified Ohm's Law offers a more accurate representation of thermal behavior compared to the standard version. This translates to more precise predictions of device temperature, especially during periods of rapid temperature changes. The validation process goes beyond simply establishing the Modified Ohm's Law. It provides valuable insights into the thermal dynamics of the device, allowing for the refinement of simulation parameters used to assess various cooling strategies. These strategies include simulating different heat sink geometries and materials, modifying airflow rates over the device's surface, and exploring the impact of Thermal Interface Materials (TIMs) between the device and the heat sink. By incorporating these elements, the simulations provide a more comprehensive picture of the device's thermal behavior under various operating conditions and cooling configurations. Ultimately, this paper not only advances the theoretical understanding of thermal management but also offers practical benefits. Through enabling more accurate thermal predictions, the Modified Ohm's Law model paves the way for informed decision-making in device design and optimization.

**Keywords:** Thermal management, High-power semiconductor devices, Modified Ohm's Law, Nonlinear relationship, Temperature-dependent resistance, Heat dissipation, Simulation, Thermal behavior, Accuracy, Device temperature

## 1. INTRODUCTION

High-power semiconductor devices are indispensable components in a wide array of electronic systems, spanning industries such as power electronics, automotive engineering, telecommunications, and renewable energy [1,2]. These devices serve as the backbone of modern electronic systems, facilitating the delivery of high levels of power and efficiency required to drive various applications [2]. Whether powering electric vehicles, transmitting data across telecommunications networks, or harvesting renewable energy, high-power semiconductor devices form the cornerstone of technological advancements across diverse sectors [3,4]. However, as technological advancements drive the proliferation of high-power semiconductor devices, the accompanying increase in power densities poses significant challenges in terms of thermal management [5-7]. With more power packed into smaller footprints, these devices inevitably generate substantial amounts of heat during operation [7]. Effective thermal management becomes crucial to prevent excessive heat buildup, which can compromise device performance and reliability. Without adequate cooling mechanisms in place, high temperatures can lead to thermal stress, material degradation, and ultimately, device failure [8,9]. The relentless pursuit of miniaturization and efficiency in electronic systems intensifies the need for innovative thermal management solutions. Dissipating heat effectively and maintaining temperatures within safe operating ranges is paramount for achieving optimal device performance and reliability. Therefore, thermal management becomes increasingly crucial as power densities climb to meet the demands of emerging technologies like electric vehicles, 5G telecommunication networks, and renewable energy systems [6]. The escalating power densities of high-power semiconductor devices are a direct consequence of the miniaturization trend and the drive for more efficient electronics [10,11]. As these devices evolve to meet the demands of modern technology, they can handle significantly more power within a fixed volume. However, this miniaturization with increased power density comes at a significant cost-the generation of substantial heat during operation [10]. If not managed effectively, this heat can severely impact the performance and reliability of high-power semiconductor

* Corresponding author, e-mail: alexkimuya23@gmail.com (A. M. Kımuya)
Recieved: 02.04.2024 Accepted: 24.05.2024
doi: 10.55696/ejset.1463554

devices [5]. As heat accumulates within the devices, temperatures can rise beyond safe operating limits established by manufacturers. These elevated temperatures not only degrade the immediate performance of the devices but also compromise their long-term reliability. Over time, prolonged exposure to high temperatures can accelerate device aging, degrade materials, and ultimately lead to premature device failure [5,12]. Traditional thermal management approaches often rely on basic linear models, such as Standard Ohm's Law, to predict and mitigate heat generation in semiconductor devices [13]. While these models can be adequate for low to moderate power densities, they struggle with the complexities of thermal behavior exhibited by high-power devices. Notably, linear models may neglect significant non-linear effects that become more pronounced at higher power densities [14,15]. Non-linear phenomena such as temperature-dependent changes in resistance and thermal conductivity significantly impact the thermal behavior of high-power semiconductor devices [16,19]. These non-linearities cause deviations from linear model predictions, rendering them insufficient for accurate thermal modeling and management in high-power applications. Consequently, the need for more sophisticated thermal management techniques that account for these non-linear effects and provide more accurate performance and reliability predictions has become increasingly recognized. This paper proposes a novel method for managing heat in high-power semiconductor devices. It focuses on using a modified version of Ohm's Law to address this challenge empirically. This modified version incorporates the exponential relationship between temperature, resistance, and current. The objective is to offer a more precise and reliable way to model the thermal behavior of these devices. Through empirical validation and simulations, we aim to demonstrate how this Modified Ohm's Law can improve cooling strategies and mitigate thermal issues in high-power semiconductor devices. The paper establishes the first empirical applications of the Modified Ohm's Law in addressing thermal management challenges in high-power semiconductor devices. A comprehensive framework integrating theoretical insights with practical experimentation advances understanding of thermal dynamics and facilitates more effective cooling strategies. The benefits of employing the Modified Ohm's Law instead of traditional linear models are elucidated to aid in advancing thermal management techniques. By delving into the theoretical underpinnings of the Modified Ohm's Law, outlining the methodology for empirical validation, presenting simulated experiments, and discussing the implications of findings, a holistic understanding of its role in addressing thermal management challenges and unlocking the full potential of high-power semiconductor devices in diverse electronic applications is provided.

## 2. LITERATURE REVIEW

Thermal management in high-power semiconductor devices is a critical aspect of modern electronics, with various approaches and models developed to address associated challenges. This section provides an overview of current approaches, identifies their limitations, and highlights the need for innovative solutions to optimize device performance and reliability.

### 2.1 Historical Context

Early efforts in thermal management focused on developing basic heat dissipation techniques to combat rising temperatures in semiconductor devices [20-23]. The primary concern during this period was preventing overheating and ensuring reliable operation of electronic components. Simple solutions like heat sinks and fans became the workhorses of thermal management, dissipating heat generated by high-power devices to minimize thermal damage and extend the lifespan of semiconductor systems [23-25]. These pioneering thermal management techniques were the first steps towards addressing the thermal challenges of high-power devices. Through implementing these fundamental yet effective heat dissipation mechanisms, engineers laid the groundwork for the development of more sophisticated thermal management strategies in the years to come [26,27]. These foundational techniques not only helped mitigate immediate thermal concerns but also paved the way for more advanced cooling solutions as power densities continued to increase [26]. Through empirical experimentation and iterative refinement, engineers gained valuable insights into the thermal behavior of semiconductor devices and the effectiveness of different cooling methods. This period of experimentation and innovation laid the groundwork for the evolution of thermal management practices, providing a foundation for the development of more comprehensive and efficient cooling strategies in the future [20,28,29].

### 2.2 Current Approaches

Current thermal management practices for high-power semiconductor devices often rely on simplistic models, with a primary focus on the Standard Ohm's Law for temperature prediction and cooling strategy development [30]. This approach treats thermal behavior as a linear relationship between temperature (T), thermal resistance ($R_{th}$), and current (I). However, recent research highlights the limitations of these linear models in capturing the complexities of heat generation and transfer within high-power devices [31-33]. For instance, studies on power electronics modules have shown that thermal resistance is not constant, but rather increases as temperature rises [34,35]. This non-linearity can significantly affect temperature predictions based on the Standard Ohm's Law, potentially leading to underestimates of heat generation and overestimates of cooling effectiveness. Consequently, overdependence on linear models can result in suboptimal cooling solutions, as evidenced by cases where high-power LED

arrays experienced overheating and reduced lifespan due to inaccurate thermal management strategies [36]. These limitations become even more critical as power densities continue to increase and operating conditions become more dynamic. In high-power applications like data centers and electric vehicles, where precise thermal control is crucial for performance and reliability, linear models may struggle to predict temperature variations accurately, potentially leading to thermal runaway and device failure as discussed by [37].

### 2.3 Limitations of Current Approaches

Thermal management of high-power semiconductor devices faces several limitations with the rise of complex operating environments. While existing approaches offer a foundation, they often struggle to keep pace with the evolving demands of these devices.

A key constraint lies in the extensive use of linear models, like those derived from Standard Ohm's Law, to predict thermal behavior [1,2]. These models offer advantages in their simplicity and ease of implementation. However, they inherently disregard the non-linear effects caused by temperature dependence of resistance. This becomes particularly problematic in high-power devices that experience dynamic operating conditions and inevitable temperature fluctuations. A study by [38] demonstrated that neglecting such non-linear behavior in a high-power GaN transistor model led to significant underestimation of junction temperatures, potentially resulting in device failure under high-stress operating conditions.

Furthermore, commonly employed empirical methods in thermal management can lack the precision needed to capture the nuances of thermal behavior under diverse operating conditions. These approaches often rely on experimental data obtained from limited scenarios, such as specific power levels or ambient temperatures [22,25,28,29]. This limited data set fails to capture the complex thermal dynamics encountered in real-world applications, where various environmental factors like fluctuating power loads and changing ambient conditions can significantly impact device temperature. For instance, a study by [39] compared various empirical thermal models for a high-power IGBT module and found that all models exhibited significant deviations from experimental data at operating conditions beyond the limited range used to generate the empirical correlations. This highlights the limitations of such methods in accurately predicting device temperatures across a wide range of operating scenarios.

Current approaches also struggle to adapt to the ever-increasing diversity of operating conditions and device geometries encountered in high-power semiconductor applications [6,8,13,19]. These devices often operate in environments with significant variations in ambient temperature, power levels, and physical configurations. Failing to account for these variations can lead to thermal management strategies that are poorly suited to the specific needs of a device, potentially compromising its performance and reliability. For example, a study by [40] investigated the thermal performance of a high-power LED array under varying operating currents. The results showed that a thermal management strategy designed based on a constant operating current proved inadequate when the current was dynamically adjusted. This emphasizes the need for more adaptable thermal management approaches that can account for the diverse operating conditions experienced by high-power semiconductor devices.

### 2.4 Emerging Trends and Technologies

Recent advancements in materials science and computational modeling have revolutionized the field of thermal management, offering innovative solutions to the challenges posed by high-power semiconductor devices. These advancements play a significant role in improving thermal management techniques and optimizing device performance, as highlighted by [41,42].

**Materials Science Advancements.** One of the most exciting frontiers in thermal management for high-power electronics lies in the development of novel materials with exceptional thermal properties. These advancements are crucial for mitigating heat buildup and ensuring optimal device performance ([41,42]). A key area of focus is nanomaterials, particularly graphene and carbon nanotubes. These materials boast remarkably high thermal conductivity, surpassing traditional materials like copper by several orders of magnitude ([43,44]). This translates to significantly more efficient heat transfer within semiconductor devices. For example, studies have demonstrated that incorporating graphene films into device packaging can significantly reduce temperature gradients across the chip [45,46]. This translates to a two-fold benefit-improved device reliability by mitigating localized overheating and enabling miniaturization of electronic components due to more efficient heat dissipation.

Beyond graphene and carbon nanotubes, researchers are actively exploring other promising materials like diamond and boron nitride for their exceptional thermal conductivity. Additionally, the development of composite materials that combine high thermal conductivity fillers with polymer matrices offers a path towards creating lightweight and flexible heat dissipation solutions for various applications ([47,48]). These advancements in materials science are fundamentally transforming thermal management strategies, paving the way for a new generation of high-performance and reliable electronic devices.

**Computational Modeling.** Advancements in computational modeling have revolutionized the approach to thermal management for high-power semiconductor devices. These advancements empower engineers with powerful tools to analyze and predict thermal behavior within the devices with unprecedented detail. Finite element analysis (FEA) and computational

fluid dynamics (CFD) techniques have become the cornerstones of this revolution, playing a critical role in optimizing device performance and developing effective cooling strategies [49,50].

FEA excels at simulating heat transfer within complex geometries of semiconductor devices. By discretizing the device into a mesh of elements, FEA software can calculate temperature distribution throughout the device under various operating conditions. This allows engineers to identify potential thermal hotspots and assess the effectiveness of different heat sink designs. For instance, a study by [51] employed FEA to simulate the thermal performance of a novel microchannel heat sink design for a high-power LED array. The simulation results guided the optimization of the microchannel geometry, leading to a significant reduction in junction temperature compared to conventional heat sink designs [51].

On the other hand, CFD simulations excel at modeling fluid flow and heat transfer across surfaces. This capability is crucial for analyzing the performance of various cooling systems, such as forced convection cooling using fans or liquid cooling with microfluidic channels. For example, a study by [52] utilized CFD simulations to evaluate the thermal performance of a microfluidic cooling system for a high-power processor. The simulations enabled the researchers to optimize the flow path design within the microchannels, achieving a substantial improvement in heat dissipation from the processor.

By leveraging these computational modeling tools, engineers can explore a vast design space virtually. They can experiment with different materials, device geometries, and cooling system configurations without the need for expensive physical prototypes. This iterative design process facilitated by simulation software significantly reduces development time and cost while optimizing thermal management solutions for specific device requirements.

**Novel Cooling Techniques.** While advancements in materials and modeling offer significant improvements, novel cooling techniques are emerging to address the thermal challenges of high-power semiconductor devices. These techniques often push the boundaries of conventional heat dissipation methods. One such promising approach utilizes phase-change materials (PCMs) [53,54]. PCMs exhibit a unique property-they can reversibly transition between solid and liquid states. During this phase change, PCMs absorb or release significant amounts of latent heat, acting as a thermal buffer. This makes them ideal for thermal energy storage and passive cooling applications in electronic devices [54]. For instance, a PCM could be embedded within the device packaging or heat sink. As the device heats up, the PCM absorbs the excess heat by melting. When the device cools down, the PCM solidifies again, releasing the stored thermal energy. This cycle can be repeated, providing a passive and localized cooling mechanism that helps to regulate device temperature. Through incorporating these innovative materials and exploring other emerging methods, researchers are continuously seeking to improve thermal management strategies for high-power electronics, ensuring optimal device performance and reliability.

**Microfluidic Cooling Systems.** Microfluidic cooling systems are rapidly gaining traction as a promising alternative to conventional air or liquid cooling methods for high-power semiconductor devices. These systems take advantage of microfabrication techniques to integrate miniature channels, typically ranging from 10 to 100 micrometers in width, directly within the silicon substrate of the device. Coolant, such as water or a dielectric fluid, is then circulated through these microchannels. This design offers several advantages over traditional cooling methods. Due to the close proximity of the microchannels to heat sources within the device, microfluidic cooling enables highly efficient heat removal from localized hotspots. This translates to a more uniform temperature distribution across the device compared to conventional cooling approaches where heat transfer is less efficient. The improved thermal management provided by microfluidic cooling allows for significant performance benefits. Studies have shown that microfluidic cooling can lead to substantial reductions in junction temperatures, enabling higher clock speeds and improved device reliability [55,56]. For instance, research by [52] demonstrated a microfluidic cooling system that achieved a 44.4% reduction in peak junction temperature compared to a conventional air-cooled system, allowing the device to operate at a significantly higher clock speed. These advancements highlight the potential of microfluidic cooling to revolutionize thermal management strategies for next-generation high-power electronics.

### 2.5 Relevance to the Current Study

This section underscores the critical need to overcome limitations in current thermal management techniques for high-power semiconductor devices. Prior research has highlighted the shortcomings of linear models like Ohm's Law in accurately predicting thermal behavior under dynamic conditions. These models often neglect non-linear effects such as temperature-dependent resistance variations, which can negatively impact device performance and reliability. Conversely, research suggests promise in innovative approaches like the Modified Ohm's Law for addressing these challenges. By incorporating non-linear relationships between temperature, resistance, and current, the Modified Ohm's Law offers a more comprehensive framework for modeling thermal behavior in high-power devices [37]. Building on this foundation, this study aims to empirically validate the application of the Modified Ohm's Law for optimizing cooling strategies in high-power semiconductor devices. Through rigorous simulation experiments and analysis, this paper intend to demonstrate the effectiveness of the Modified Ohm's Law in accurately predicting thermal behavior and guiding the design of efficient cooling solutions. Leveraging insights from previous research and emerging technologies, our study contributes to advancements in thermal management within the field of electronics.

# 3. METHODOLOGY

This section presents a methodology aimed at validating the Modified Ohm's Law using simulated experiments, with a specific focus on its efficacy in managing thermal problems in high-power semiconductor devices. To achieve this goal, essential parameters such as temperature profiles, resistance variations, and current flows will be defined, forming a solid basis for simulating thermal dynamics. Subsequently, a simulation framework is developed, incorporating both Standard Ohm's Law and Modified Ohm's Law principles. Utilizing computational techniques, this framework will be fine-tuned to replicate real-world device characteristics. Through a series of simulated experiments encompassing diverse power levels, temperature gradients, and device geometries, a comparative analysis will be conducted to assess the predictive capabilities of the Standard Ohm's Law and Modified Ohm's Law in thermal management and cooling optimization. This analysis aims to elucidate how well the Modified Ohm's Law aligns with conventional expectations and its potential to enhance device performance and reliability.

### 3.1 Validation of Modified Ohm's Law through Simulated Experiments

This section describes the implementation of simulated experiments designed to validate the effectiveness of the Modified Ohm's Law in capturing the thermal behavior of high-power semiconductor devices compared to the Standard Ohm's Law. The section leverage the fundamental ingredients established in Appendix IV-Establishing a Simulation Framework to achieve this goal.

#### 3.1.1 Simulation Environment Setup

We establish a framework that replicates real-world conditions experienced in high-power electronic systems, drawing upon the geometric parameters and material properties outlined in Appendix IV. This includes aspects like device geometry, substrate properties, and heat sink design. The methods for modeling heat transfer within the device and defining boundary conditions, such as ambient temperature, are rigorously defined. To model heat transfer accurately, we leverage principles from the field of computational fluid dynamics (CFD) [49,50]. Specifically, we employ the finite element method (FEM), a well-established numerical technique for solving the partial differential equations that govern heat conduction in solids [49]. The governing equation for heat conduction, often referred to as the heat equation, is expressed in Equation (1).

$$\frac{\partial T}{\partial t} = \alpha \nabla^2 T \tag{1}$$

Where $T$ is the temperature distribution within the semiconductor device, $t$ is time, $\alpha$ is the thermal diffusivity of the material, and $\nabla^2$ is the Laplacian operator representing the spatial variation of temperature. Equation (1) describes how temperature changes over time due to heat diffusion within the material.

In addition to modeling heat conduction within the device, we define boundary conditions to simulate heat transfer at device interfaces. These conditions dictate the temperature and heat fluxes at the device's boundaries, including its contact with the surrounding environment. For instance, at the interface between the device and the heat sink, we may specify a convective heat transfer boundary condition to account for the cooling effect of airflow. This approach aligns with Newton's law of cooling, which describes how heat is transferred from the device to the surrounding environment via convection [57]. Mathematically, this boundary condition can be expressed as Equation (2).

$$q = h(T - T_{ambient}) \tag{2}$$

Where $q$ is the heat flux, $h$ is the convective heat transfer coefficient, $T$ is the temperature at the device surface, and $T_{ambient}$ is the ambient temperature. This equation represents Newton's law of cooling and describes how heat is transferred from the device to the surrounding environment via convection. While Equation (2) explicitly represents the boundary condition, the actual implementation within the simulation process (described in the following section) utilizes implicit Dirichlet boundary conditions $T(0) = T_{ambient}$ and $T(L) = T_{hot}$ at the ends of the device [58,59]. This enforces specific temperature values at these designated locations.

#### 3.1.2 Implementation of Standard and Modified Ohm's Law

This section involves the methodology for integrating both the standard and Modified Ohm's Laws applications into the simulation environment. Consider the following computational steps.

To solve equation (1) which represents the one-dimensional heat conduction equation, we will discretize the domain into $N_x$ spatial grid points $x_i$ where $i = 1,2,3, \dots N_x$. This allows us to approximate the spatial derivatives using finite differences. Let $\Delta x$ be the spatial step size.

We will also consider the boundary conditions provided in equation (3).

- Dirichlet boundary conditions. $T(0) = T_{ambient}$ and $T(L) = T_{hot}$ (3)

To proceed, we approximate the second spatial derivative $\nabla^2 T$ using central finite differences with respect to spatial coordinate $x$ as expressed in equation (4).

$$\frac{\partial^2 T}{\partial x^2} \approx \frac{T_{i+1} - 2T_i + T_{i-1}}{\Delta x^2} \quad (4)$$

Using the finite element method, we approximate the temperature field $T(x)$ as a linear combination of basis functions over finite elements.

Denote $N_n$ to be the total number of nodes.

Then, we have:

$$T(x) \approx \sum_{j=1}^{N_n} N_j(x) \cdot T_j \quad (5)$$

Where $N_j(x)$ is the shape function associated with node $j$, and $T_j$ is the temperature at node $j$.

Substituting the discretized second derivative and the FEM approximation into equation (1), we obtain a system of ordinary differential equations (ODEs) for each node $i$ through equation (6).

$$\frac{\partial T_j}{\partial t} = \alpha \cdot \frac{T_{i+1} - 2T_i + T_{i-1}}{\Delta x^2} \quad (6)$$

Substituting this approximation into the one-dimensional heat conduction equation ($\frac{\partial T}{\partial t} = \alpha \frac{\partial^2 T}{\partial x^2}$);

We get:

$$\frac{T_i^{(n+1)} - T_i^{(n)}}{\Delta t} = \alpha \cdot \frac{T_{i+1}^{(n)} - 2T_i^{(n)} + T_{i-1}^{(n)}}{\Delta x^2} \quad (7)$$

Where $T_i^{(n)}$ represents the temperature at spatial point $x_i$ and time step $n$, and $\Delta t$ is the time step size.

### 3.1.3 Solver Implementation Algorithm

The finite difference equation can be solved iteratively using various numerical integration methods. These methods include the explicit or implicit Euler method, Runge-Kutta methods, and the Crank-Nicolson method [60-62]. In this paper, we prioritize computational efficiency by selecting the explicit Euler method. This method is a popular choice due to its straightforward implementation and ease of understanding [60]. While alternative methods like the implicit Euler method and Runge-Kutta methods may offer greater accuracy, the explicit Euler method proves to be computationally less expensive [60,62,63]. This benefit is particularly relevant considering limitations in our available computational resources. Additionally, the explicit Euler method's clear and simple implementation makes it well-suited for solving the finite difference equation within this context.

**Boundary Conditions.** We apply the Dirichlet boundary conditions established in equation (3); $T(0) = T_{ambient}$ and $T(L) = T_{hot}$ which specify the temperatures at the ends of the semiconductor device. These conditions specify the temperatures at the boundaries of the device, allowing us to capture the heat transfer occurring between the device and its surroundings.

**Material Properties and Geometric Parameters.** We define the material properties such as thermal conductivity $k(x)$ and geometric parameters like the device length $L$. These parameters are crucial for accurately modeling heat conduction within the device and determining its thermal behavior.

**Application of Ohm's Laws.** Once we have obtained the temperature distribution $T(x)$, we apply Ohm's Laws to calculate the current passing through the device. For the Standard Ohm's Law $= {}^{V}/_{R}$, we assign a constant resistance value based on the chosen material properties at a specific reference temperature. The Modified Ohm's Law for this application expressed as; $\left(I_{modified} = a \times e^{\frac{R_{short}}{R_0} \times \frac{x}{L}}\right)$ is integrated into the solver to account for the temperature dependence of resistance. Where $V$ is the voltage, $R$ is the resistance, $a$ is a constant, $R_0$ is the reference resistance, $R_{short}$ is the short resistance, and $x$ is the spatial coordinate.

These steps constitute the solver algorithm for effectively simulating heat conduction within the semiconductor device, incorporating boundary conditions, material properties, geometric parameters, and the application of Ohm's Laws to accurately capture its thermal behavior. The solver algorithm is implemented according to the computation provided in Appendix I, ensuring a systematic approach to simulate heat conduction within the semiconductor device.

### 3.2 Simulation Experiment Design

#### 3.2.1 Simulation and Design for Thermal Analysis of Semiconductor Devices

For the thermal analysis of semiconductor devices, the simulation experiment design employed a Monte Carlo simulation approach for synthetic data generation. This method was chosen due to its capability of systematically exploring a vast range of potential operating conditions by introducing perturbations within predefined ranges for material properties and boundary conditions [64]. Leveraging this technique, it was possible to randomly vary parameters like thermal conductivity and boundary temperatures for each sample within the simulation. This variation mimics the inherent uncertainties encountered in real-world scenarios. Subsequently, temperature distributions were computed using the Finite Element Method (FEM), enabling a detailed comprehension of the thermal behavior of the semiconductor device under various operating conditions and cooling strategies. To further enhance the realism of the synthetic data, noise was incorporated into the temperature distributions. This addition accounts for measurement errors and environmental uncertainties that may be present in real-world measurements. The provided simulations through the subsequent sections leverages the solver implementation framework outlined in Appendix I and the synthetic data generated by the simulation data generator described in Appendix II.

**Operating Conditions.** The initial step involves establishing the operating conditions for the semiconductor device simulation. These conditions encompass a range of parameters that significantly influence the temperature distribution and heat dissipation within the device. The key parameters include;

- **Power Levels.** Varying power levels simulate the device's operation under different workloads, directly impacting heat generation.
- **Heat Loads.** External heat loads represent additional heat sources that the device must dissipate, such as from surrounding components.
- **Ambient Temperatures.** Simulating different ambient temperatures reflects the device's operating environment and its effect on heat transfer.

Through varying these operating conditions, the simulation observes their impact on the thermal performance of the semiconductor device. This allows for the evaluation of different cooling strategies' effectiveness in maintaining optimal operating temperatures.

**Cooling Strategies.** The simulation experiment subsequently explores various cooling strategies employed to mitigate heat buildup within the device. These strategies encompass a range of techniques that enhance heat transfer from the device to its surroundings.

- **Airflow Rates.** Modifying the airflow rate over the device's surface influences convective heat transfer.

- **Heat Sink Configurations.** Simulating different heat sink geometries and materials evaluates their effectiveness in conducting heat away from the device.

- **Thermal Interface Materials (TIMs).** Varying the TIM properties between the device and the heat sink affects the thermal conductivity at the interface, impacting heat transfer.

The simulation process involves implementing these cooling strategies within the solver framework. The resulting data from each simulation run allows for the assessment of each cooling method's ability to effectively dissipate heat and maintain optimal operating temperatures for the semiconductor device.

**Validation Metrics.** To compare the results obtained with both the standard and Modified Ohm's Law versions, the experiment defines crucial validation metrics. These metrics serve as quantitative measures for evaluating the accuracy and reliability of the Modified Ohm's Law in predicting the thermal behavior of the semiconductor device compared to the traditional approach. The key validation metrics include;

- **Temperature Distribution.** The temperature distribution within the device provides a detailed picture of hot and cold spots, crucial for identifying potential thermal risks.

- **Maximum Device Temperature.** The peak temperature reached during operation is a critical parameter as it determines the device's reliability and performance.

- **Power Dissipation.** The power dissipated by the device represents the amount of heat it generates, which needs to be effectively managed by the cooling system.

Through analyzing these metrics for simulations run with both standard and Modified Ohm's Law implementations, the experiment aims to establish a clear understanding of the modified Law's effectiveness in accurately predicting the thermal behavior of the semiconductor device. The subsequent section presents the detailed results obtained from the simulation experiments.

## 4. SIMULATION ANALYSIS AND RESULTS

This section presents the results obtained from the simulation experiments designed to evaluate the thermal behavior of the semiconductor device under various operating conditions and cooling strategies. The analysis focuses primarily on the temperature distribution within the device, a critical factor impacting its performance and reliability.

### 4.1 Temperature Profiles Using Temperature-Dependent Resistance Models

A crucial aspect of the simulation analysis involves comparing the temperature profiles obtained with both the standard and Modified Ohm's Law implementations. This comparison highlights the impact of incorporating the non-linear behavior of resistance in the modified Law on the predicted temperature distribution. The simulations were conducted across a range of operating conditions, including varying power levels, heat loads, and ambient temperatures. The results consistently demonstrate noticeable differences in the temperature profiles predicted by the two versions of Ohm's Law.

#### 4.1.1 Power Levels

Simulations were conducted using varying power densities to analyze their impact on the temperature distribution within the device, as shown in Figure 1. The results confirm that for both Standard Ohm's Law and Modified Ohm's Law, increasing power densities lead to a rise in temperature throughout the device. However, Figure 1 also reveals that the Modified Ohm's Law consistently predicts slightly higher temperatures compared to the standard approach. The observed discrepancy can be attributed to the non-linear dependence of resistance on temperature incorporated into the Modified Ohm's Law. As the power density increases within the device, so too does the temperature. This rise in temperature results in a greater increase in resistance for the Modified Ohm's Law compared to the Standard Ohm's Law, as evidenced by the wider temperature contours in the Modified Ohm's Law plots of Figure 1. The increased resistance leads to a more significant Joule heating effect, causing a higher predicted temperature according to the Modified Ohm's Law. This effect is most pronounced at higher power densities (300 $W/mm^2$), where the temperature difference between the two approaches is greatest. A notable observation in Figure 1 is that the hottest region in the temperature distribution for (300 $W/mm^2$) using the Modified Ohm's Law appears narrower compared to the other cases. This could be due to the following two factors:

- The non-linear effect of temperature on resistance can lead to a sharper temperature gradient near the heat source in the Modified Ohm's Law case, resulting in a narrower hot zone.

- Numerical discretization artifacts inherent to the applied finite difference method might also play a minor role. Further simulations with a finer mesh could be conducted to investigate this possibility, in a separate study.

According to Figure 1, the simulations demonstrate the significant impact of incorporating temperature-dependent resistance into the model. The Modified Ohm's Law predicts a more realistic temperature distribution within the device, particularly at higher power densities.

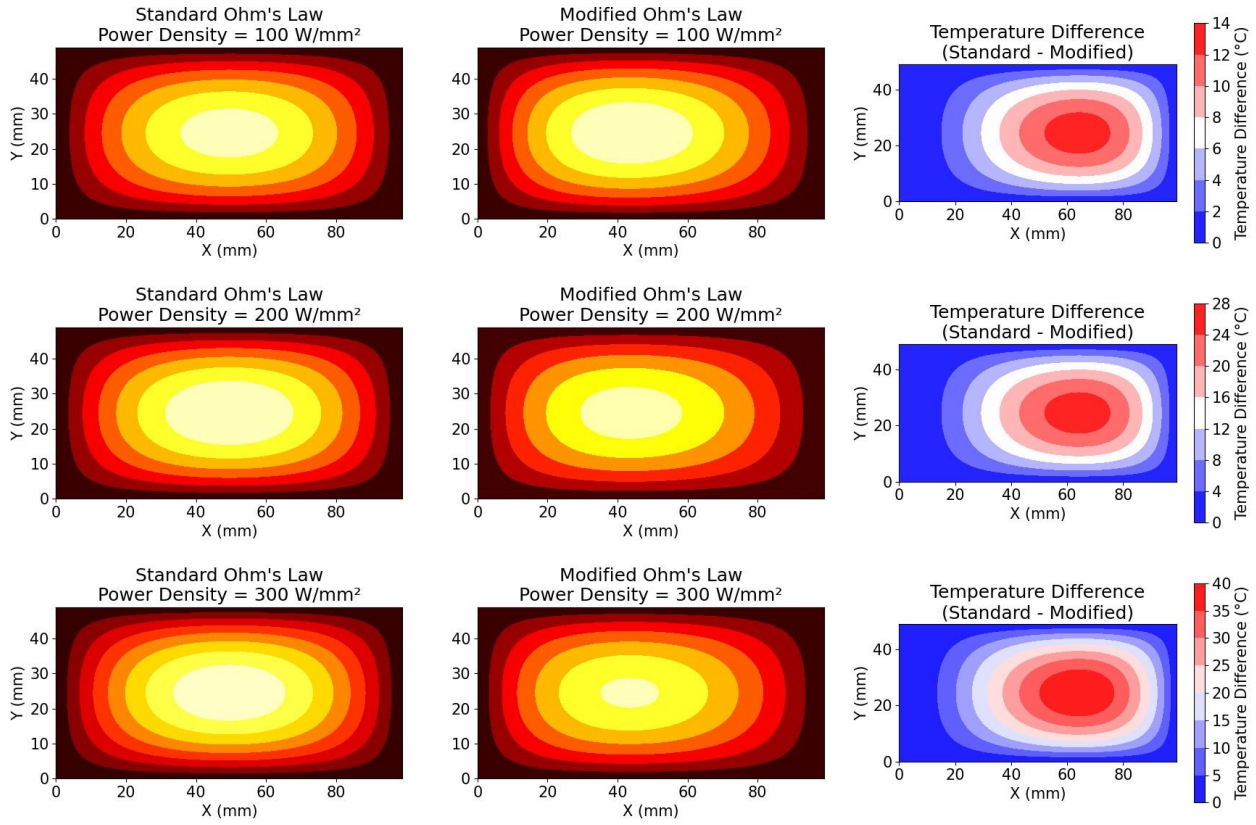


**Figure 1.** Temperature Distribution within the Device at Varying Power Densities. (*The figure shows the temperature distribution within the device under three different power densities (100 $W/mm^2$, 200 $W/mm^2$, and 300 $W/mm^2$) for both standard and Modified Ohm's Law.*)

**Validation Remark 1**. Both the standard and Modified Ohm's Laws are applied in the simulation analysis to predict the temperature distribution within the semiconductor device. However, the discrepancy observed between the temperature profiles obtained with the two versions suggests that the temperature-dependent resistance model more accurately captures the device's thermal behavior. The incorporation of temperature-dependent resistance accounts for the non-linear relationship between temperature and resistance, which is often observed in semiconductor materials. Therefore, while both versions of Ohm's Law are used in the analysis, the temperature-dependent resistance model appears to provide a more accurate representation of the device's thermal response under varying operating conditions.

### 4.1.2 Heat Loads

In this analysis, the influence of external heat loads on temperature distribution within the device was investigated using simulations incorporating various heat loads added to the device model. As illustrated in Figure 2(a) for Standard Ohm's Law and Figure 2(b) for Modified Ohm's Law, both approaches predict a rise in temperature throughout the device due to the presence of the additional heat source. The data in both figures shows a clear trend of increasing temperature throughout the device as the external heat load increases (represented by Load in Figure 2(a) for Standard Ohm's Law). This aligns with the core principle of

Standard Ohm's Law, where $V = IR$ ($Voltage = Current\ x\ Resistance$) and the requirements of the and Modified Ohm's Law provided by [37]. The addition of an external heat source raises the thermal energy within the device, which can be thought of as an increased difficulty for current flow. Consequently, both Ohm's Law equations would suggest a proportional rise in temperature as the device attempts to maintain its operating current under these new thermal conditions.

Standard Ohm's Law (Figure 2(a)) shows a consistent starting temperature distribution across the device, regardless of the applied heat load. This starting temperature appears to range between 0 °C and 20 °C on the Device Temperature (°C) axis. As the ambient temperature increases towards 80 °C, the temperature within the device also rises. The plot for the highest heat load (15 W) shows a temperature increase to around 100 °C on the Device Temperature (°C) axis.

For Modified Ohm's Law (Figure 2(b)), as the ambient temperature increases towards 80 °C, the temperature within the device also rises. However, the starting point for the temperature profiles is noticeably higher compared to the Standard Ohm's Law results. The plot for the lowest heat load (5 W) shows a temperature increase to around 100 °C on the Device Temperature (°C) axis, with all other temperature scenarios exceeding this value. This difference can likely be attributed to the inclusion of the temperature dependence of resistance in the Modified Ohm's Law model, which is not captured by Standard Ohm's Law.

A key distinction between Standard and Modified Ohm's Law lies in how they treat resistance. Standard Ohm's Law assumes a constant resistance value, while Modified Ohm's Law acknowledges that resistance increases as the temperature within the device rises due to the external heat load. This difference is reflected in the results. The Modified Law predicts slightly higher temperatures than the Standard Ohm's Law under similar conditions. As observed in Figure 2(b), the temperature profiles for all three heat loads (5 W, 10 W, and 15 W) on the Device Temperature (°C) axis start at a higher baseline temperature compared to Figure 2(a) for Standard Ohm's Law. Additionally, nearly all three profiles reach a temperature of 100 °C on the Device Temperature (°C) axis at the same ambient temperature (around 80 °C), whereas only the highest heat load (15 W) achieves this temperature in Figure 2(a). This observation further reinforces the notion that Modified Ohm's Law predicts a greater overall temperature rise within the device due to the temperature dependence of resistance. By incorporating this dependence, Modified Ohm's Law predicts a more pronounced temperature rise within the device under increasing external heat loads compared to Standard Ohm's Law. This highlights the importance of considering the non-linear relationship between resistance and temperature for accurate thermal modeling in semiconductor devices.

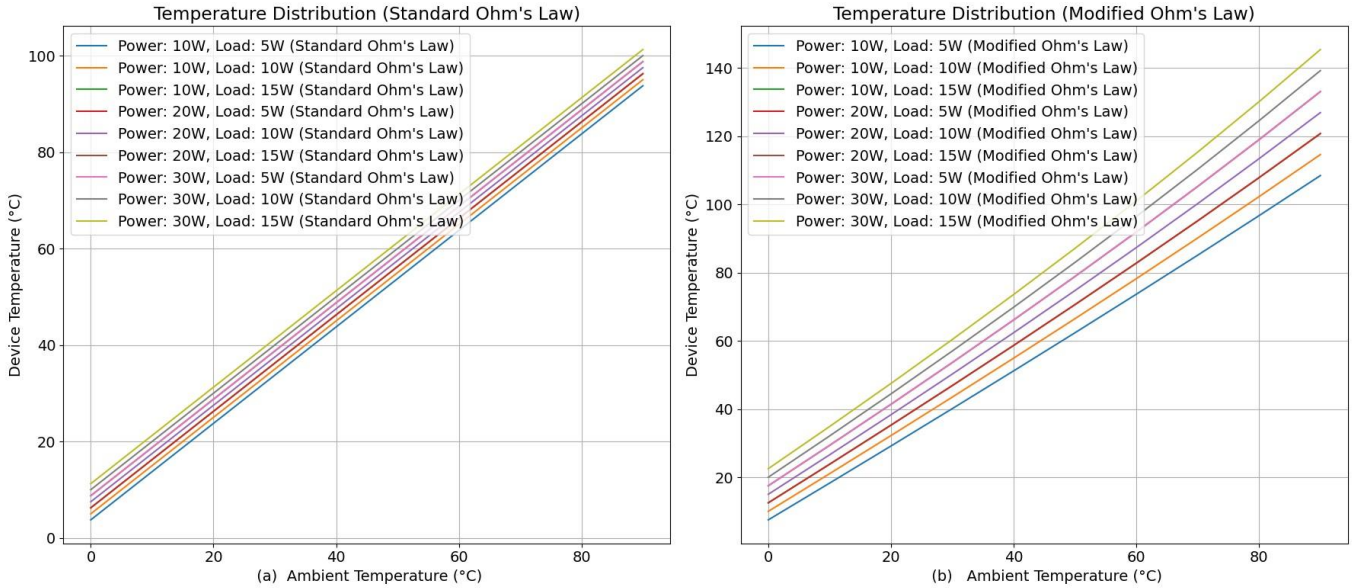


**Figure 2.** Temperature distribution analysis comparing Standard Ohm's Law (Figure 2(a)) and Modified Ohm's Law (Figure 2(b)) under varying heat loads. (The results illustrate the temperature rise within the semiconductor device as ambient temperature increases, with Modified Ohm's Law (Figure 2(b)) showing higher temperatures due to the incorporation of temperature-dependent resistance).

**Validation Remark 2**. The simulations demonstrate the importance of considering the temperature dependence of resistance in thermal modeling of semiconductor devices. Standard Ohm's Law assumes a constant resistance, which can lead to underestimating temperature rise within the device, particularly under increasing heat loads. In contrast, the Modified Ohm's Law incorporates this temperature dependence, resulting in a more accurate prediction of the temperature distribution. As observed in the simulations (Figure 1 and Figure 2), the modified Law predicts slightly higher temperatures and a more

pronounced temperature rise compared to the standard approach. This highlights the significance of accounting for the non-linear relationship between resistance and temperature for reliable thermal modeling. By validating the Modified Ohm's Law for this application, we gain a more comprehensive understanding of the thermal behavior in semiconductor devices. This knowledge is crucial for designing efficient cooling strategies to manage heat buildup and ensure optimal device operation.

### 4.1.3 Cooling Strategies and Thermal Performance Optimization

The primary objective of this section is to investigate and analyze different cooling strategies for semiconductor devices to optimize their temperature under varying ambient conditions. Specifically, the study aims to explore the effectiveness of different heat sink configurations and thermal interface materials in dissipating heat from the semiconductor device. Additionally, the study seeks to compare the thermal performance of the device using both the Finite Element Method (FEM) and standard/Modified Ohm's Law approaches to provide comprehensive insights into the effectiveness of each cooling strategy. Various parameters and configurations were defined to set the stage for the simulation. These include the ambient temperature range, representing the spectrum of environmental conditions under which the semiconductor device operates. Additionally, different heat sink configurations and thermal interface materials were identified to assess their impact on heat dissipation. Constants related to the semiconductor device, such as its physical dimensions (length, width) and thermal properties (thermal conductivity, thermal resistances), were also defined to establish the baseline for the simulations. The simulation process utilized the Finite Element Method (FEM) to simulate cooling strategy optimization. This function calculated the device temperature for various combinations of heat sink configurations and thermal interface materials. Through systematically iterating through different scenarios, the simulation provided a comprehensive understanding of how different cooling strategies influence device temperature under varying ambient conditions. Following the simulation, the obtained results are as depicted in Figure 3, which illustrates the device cooling temperature profiles for both standard and Modified Ohm's Laws using FEM. The results demonstrate how device temperature varies with ambient temperature for each cooling strategy between the Standard Ohm's Law application and the Modified Ohm's Law application.

**Analysis of Device Temperature Profiles.** The analysis of device temperature profiles for Standard and Modified Ohm's Laws provides valuable insights into the thermal behavior of semiconductor devices under varying ambient conditions. In Figure 3, the device temperature profiles for both Standard and Modified Ohm's Laws are depicted, offering a comparative view of their effectiveness in modeling heat dissipation.

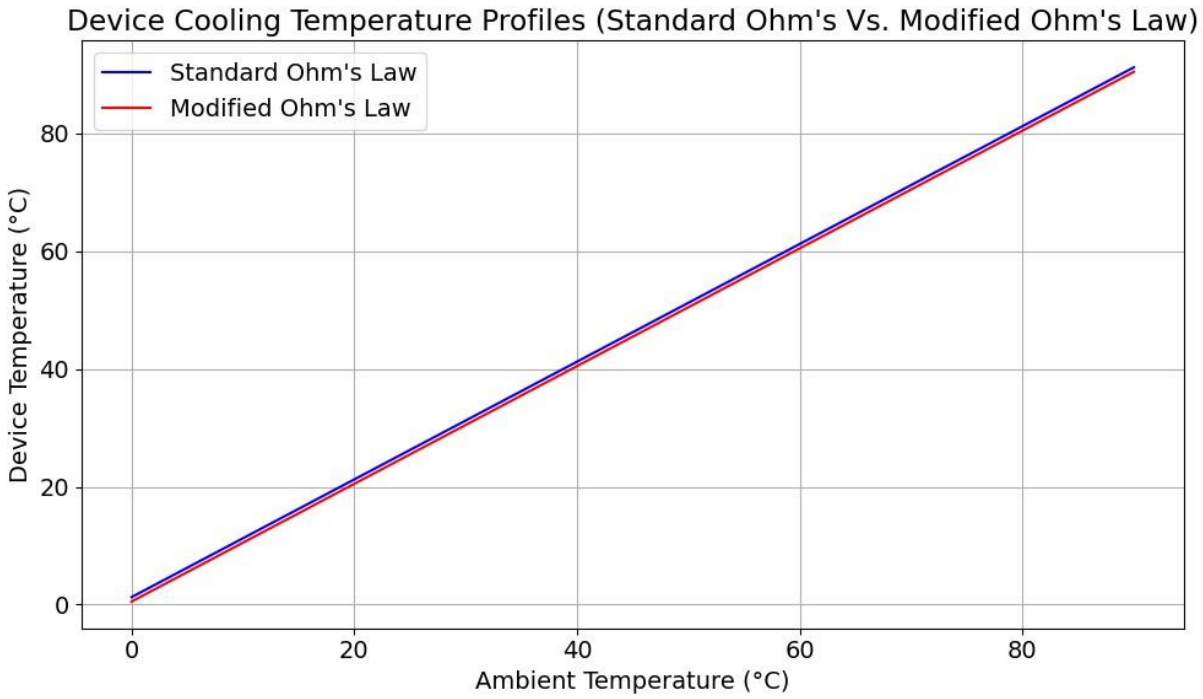


**Figure 3**. Device temperature profiles for Standard and Modified Ohm's Laws. (The Standard Ohm's Law (blue) line shows a linear increase in device temperature with rising ambient temperature, while the Modified Ohm's Law (red) line demonstrates a non-linear relationship with a steeper slope at lower temperatures and a more gradual increase at higher temperatures).

The Standard Ohm's Law analysis exhibits a linear increase in device temperature with rising ambient temperature. This linear relationship suggests a constant proportionality between the two variables, which deviates from the actual behavior observed in semiconductor devices. In reality, as the ambient temperature increases, the rate of heat transfer from the device to the environment also increases. However, this trend is not accurately captured by the Standard Ohm's Law line. Conversely, the Modified Ohm's Law demonstrates a non-linear relationship between device temperature and ambient temperature. It begins with a steeper slope at lower temperatures, indicating more rapid heat dissipation, and then transitions to a more gradual increase in a linear fashion at higher temperatures. This non-linear behavior better reflects the actual characteristics of semiconductor devices, where heat dissipation becomes more efficient at higher temperatures due to factors such as increased convection. Assuming zero temperature as the reference point, both the standard and Modified Ohm's Law curves approach zero temperature as the ambient temperature approaches zero. This observation suggests that the Modified Ohm's Law model is capable of predicting very low device temperatures, aligning with real-world scenarios. Moreover, in Appendix III, Figure 10 offers additional insights by delineating the temperature prediction differences or margins between standard and Modified Ohm's Laws. This result elucidates any discrepancies or advantages associated with each cooling strategy, facilitating the selection of the most suitable approach for optimizing device temperature and enhancing clarity in decision-making processes.

**Cooling Strategy Optimization Using Standard and Modified Ohm's Laws.** This section provides the analysis of the cooling strategy optimization for semiconductor devices based on both the Standard Ohm's Law and the Modified Ohm's Law, as illustrated in Figures 4(a) and 4(b) respectively. The visualization of device temperature profiles in Figure 4(a) under the framework of Standard Ohm's Law reveals critical insights into cooling strategy optimization. The results demonstrates the substantial impact of cooling components, showcasing how different heat sink configurations and thermal interface materials influence device temperature. Notably, configurations featuring larger heat sinks or more thermally conductive interface materials tend to result in lower device temperatures, emphasizing the efficacy of these strategies in dissipating heat and maintaining optimal operating conditions. Moreover, the results highlights the temperature sensitivity of semiconductor devices to ambient temperature fluctuations, underscoring the necessity for effective cooling solutions, particularly in environments with elevated ambient temperatures. In contrast, Figure 4(b) presents the device temperature profiles under the Modified Ohm's Law, which introduces adjustments to the calculation of device temperature. The curves in Figure 4(b) exhibit a more non-linear behavior compared to the linear trends observed in Figure 4(a), indicating that the Modified Ohm's Law accounts for factors influencing heat transfer in a more nuanced manner. These non-linear trends, attributed to specific mathematical relationships, capture phenomena such as increased heat dissipation efficiency at higher temperatures, which are not encompassed by the Standard Ohm's Law. Consequently, the Modified Ohm's Law provides more accurate predictions of device temperature, particularly at higher ambient temperatures, enhancing the efficacy of cooling system design and ensuring devices operate within safe temperature thresholds under real-world conditions.

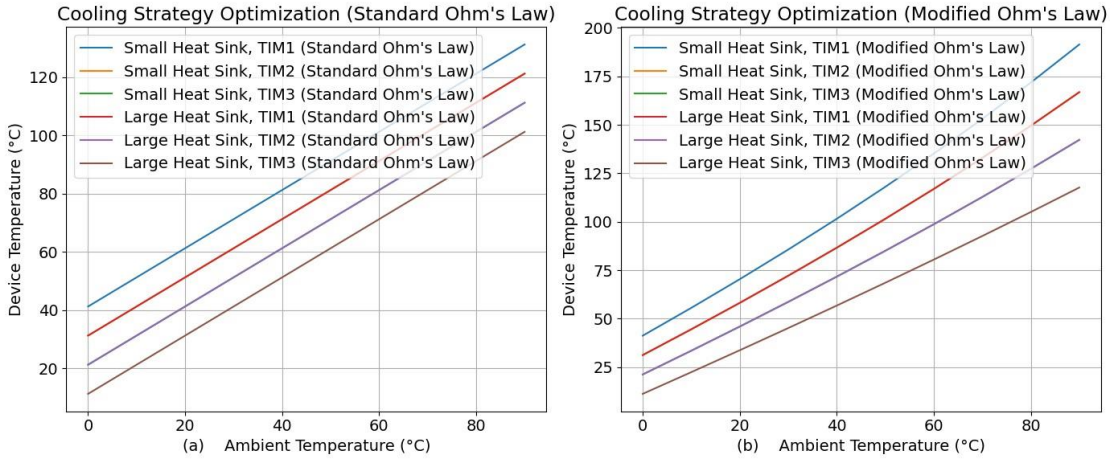


**Figure 4.** Cooling Strategy Optimization for Semiconductor Devices. (Figure (a)-Device temperature profiles for various heat sink configurations and thermal interface materials under Standard Ohm's Law. The results illustrates the impact of cooling components on device temperature, highlighting the sensitivity to ambient temperature fluctuations and the identification of optimal cooling strategies. Figure (b)-Device temperature profiles under Modified Ohm's Law, showing slight adjustments in temperature predictions compared to Standard Ohm's Law. The non-linear behavior of curves indicates sabtal factors influencing heat transfer, leading to more accurate temperature predictions, particularly at higher ambient temperatures).

Comparing the results between Figures 4(a) and 4(b), we can evaluate the efficacy of the modification introduced in Ohm's Law. This evaluation involves assessing how well the Modified Ohm's Law captures the device temperature behavior under different cooling conditions and ambient temperatures. The observed disparities in temperature trends underscore the potential advantages conferred by the Modified Ohm's Law for cooling strategy optimization, particularly in scenarios characterized by higher ambient temperatures.

**Validation Remark 3**. Based on the analysis, the Modified Ohm's Law emerges as the most suitable choice for the application of optimizing cooling strategies for semiconductor devices. The introduction of adjustments in the calculation of device temperature within the Modified Ohm's Law leads to more accurate predictions, particularly in scenarios characterized by higher ambient temperatures. The Modified Ohm's Law offers superior efficacy and reliability compared to the Standard Ohm's Law, making it the preferred choice for optimizing cooling strategies for semiconductor devices.

### 4.1.4 The Impact of Thermal Interface Materials (TIMs) on Heat Dissipation

This section presents an investigation into the impact of Thermal Interface Materials (TIMs) on the effectiveness of heat dissipation, focusing on varying TIM properties between the device and the heat sink. TIM properties significantly influence the thermal conductivity at the interface, thereby affecting heat transfer efficiency.

**Effectiveness of Heat Sink Cooling Configuration**. The investigation delves into the effectiveness of heat sink cooling configuration in light of Thermal Interface Materials (TIMs), with a specific focus on the variability of TIM properties between the device and the heat sink. Analysis of the data presented in Figure 5 reveals insights into the modeling of the cooling strategy within this context, shedding light on the suitability of the Modified Ohm's Law compared to the Standard Ohm's Law. Figure 5 underscores the pivotal role of TIM thermal conductivity in governing the heat transfer rate between the device and the heat sink. Notably, higher thermal conductivity materials correlate with lower device temperatures, while lower conductivity materials correspond to higher temperatures. This observation accentuates the significance of TIM properties in modulating the efficiency of heat dissipation mechanisms within the cooling configuration. Moreover, Figure 5 visually confirms the non-linear relationship between device current and ambient temperature, elucidating the influence of TIM properties on this dynamic. Each curve depicted in the results, representing different power densities, exhibits a non-linear increase in device current with escalating ambient temperature. This non-linearity arises from the enhanced heat dissipation observed at elevated temperatures, a phenomenon inadequately captured by the Standard Ohm's Law due to its inherent assumption of a linear current-voltage relationship.

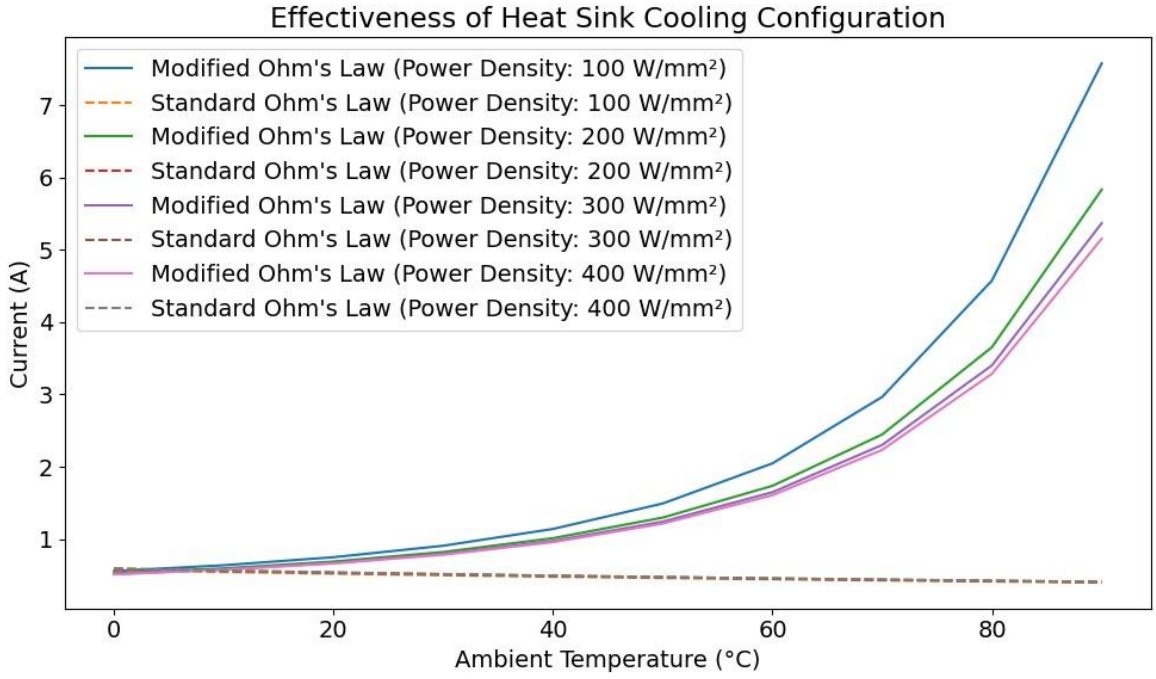


**Figure 5.** Assessment of Thermal Interface Material (TIM) Properties in Evaluating Heat Sink Cooling Configurations

The limitations of the Standard Ohm's Law become apparent within this context, as it fails to accurately model the observed non-linear trend in Figure 5. The Standard Ohm's Law's assumption of linearity between current and voltage results in a straight line representation in a current-temperature graph, which contradicts the non-linear behavior observed in the data. This discrepancy underscores the inadequacy of the Standard Ohm's Law in capturing the thermal dynamics influenced by TIM properties effectively. Conversely, the Modified Ohm's Law demonstrates greater adaptability to accommodate the non-linear heat transfer characteristics evident in Figure 5. By incorporating additional terms or equations that consider factors such as temperature-dependent thermal conductivity, the Modified Ohm's Law offers a more fitting framework for modeling the thermal behavior within the depicted cooling configuration. In scenarios where TIM properties exert a substantial influence on heat dissipation dynamics, as evidenced in Figure 5, the Modified Ohm's Law emerges as a more suitable choice for accurately representing the thermal phenomena at play.

**Effectiveness of Fun Cooling Configuration**. The analysis offers an in-depth examination of the impact of Thermal Interface Materials (TIMs) on heat dissipation effectiveness, with a specific focus on the variation in TIM properties between the device and the heat sink. Figure 6 underscores the substantial influence of TIM thermal conductivity on the heat transfer rate between the device and the heat sink. It elucidates that higher thermal conductivity materials result in lower device temperatures and correspondingly lower current, while lower conductivity materials lead to higher temperatures and higher current. This observation emphasizes the critical role of TIM properties in shaping the thermal behavior of the system. Moreover, Figure 6 depicts distinct thermal impedance characteristics, indicating a non-linear relationship between current and ambient temperature. This non-linearity arises from the improved heat dissipation observed at higher temperatures, a phenomenon not adequately captured by the Standard Ohm's Law. The limitations of the Standard Ohm's Law are highlighted within this context, as it assumes a linear relationship between current and voltage, resulting in a straight line representation in a current-temperature graph. However, the absence of such linear behavior in Figure 6 indicates a mismatch between the assumptions of the Standard Ohm's Law and the observed thermal behavior. Conversely, the Modified Ohm's Law can accommodate the non-linear heat transfer characteristics by integrating additional terms or equations that consider factors like temperature-dependent thermal conductivity. This flexibility enables the Modified Ohm's Law to provide a more accurate and comprehensive representation of the thermal behavior depicted in Figure 6.

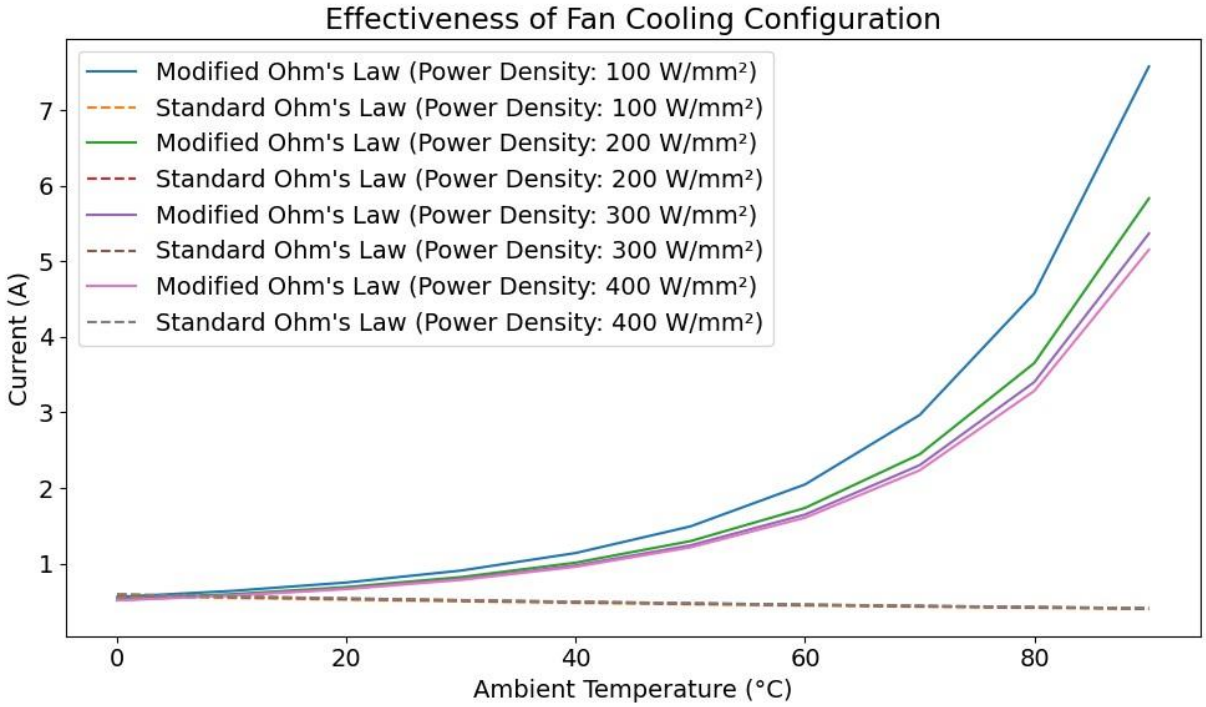


**Figure 6.** Relationship between current and ambient temperature for varying Thermal Interface Material (TIM) properties under different cooling configurations.

**Thermal Interface Materials (TIMs) Impact on Heat Dissipation Effectiveness.** This analysis sheds light on the critical role of Thermal Interface Materials (TIMs) in heat dissipation from high-power semiconductor devices. The focus lies on how variations in TIM properties between the device and the heat sink can significantly impact overall thermal performance. Figure 7 depicts a key finding-the thermal conductivity of the TIM directly affects the thermal resistance between the device and the heat sink. This resistance, in turn, influences the current flow within the system, as evident in the plotted relationship between current and ambient temperature for various TIM properties. The non-linear nature of these curves emphasizes the dynamic behavior of heat dissipation processes. Each curve exhibits a gradual increase in current at lower temperatures, followed by a steeper rise at higher temperatures. This observed non-linearity aligns closely with the predictions of the Modified Ohm's Law. The limitations of the Standard Ohm's Law become apparent in this context. It assumes a linear relationship between current and voltage, which contradicts the non-linear trends observed in Figure 7. Conversely, the Modified Ohm's Law incorporates factors like temperature-dependent thermal resistance, allowing it to account for these non-linear relationships. This adaptability makes it a more suitable choice for accurately modeling the complex thermal dynamics depicted in the figure. The visual confirmation provided by Figure 7 further reinforces the explanation. TIMs with higher thermal conductivity exhibit smaller changes in current across the temperature range. This indicates lower thermal resistance and more effective heat dissipation. Conversely, TIMs with lower thermal conductivity result in larger current variations, signifying higher thermal resistance and less efficient heat transfer. Following these results, the non-linear relationship observed in Figure 7 strongly suggests that the Modified Ohm's Law offers a more accurate representation of thermal behavior in this application compared to the standard approach. Its ability to account for temperature-dependent variations, particularly those influenced by varying TIM properties, makes it well-suited for modeling complex thermal environments in high-power semiconductor devices.

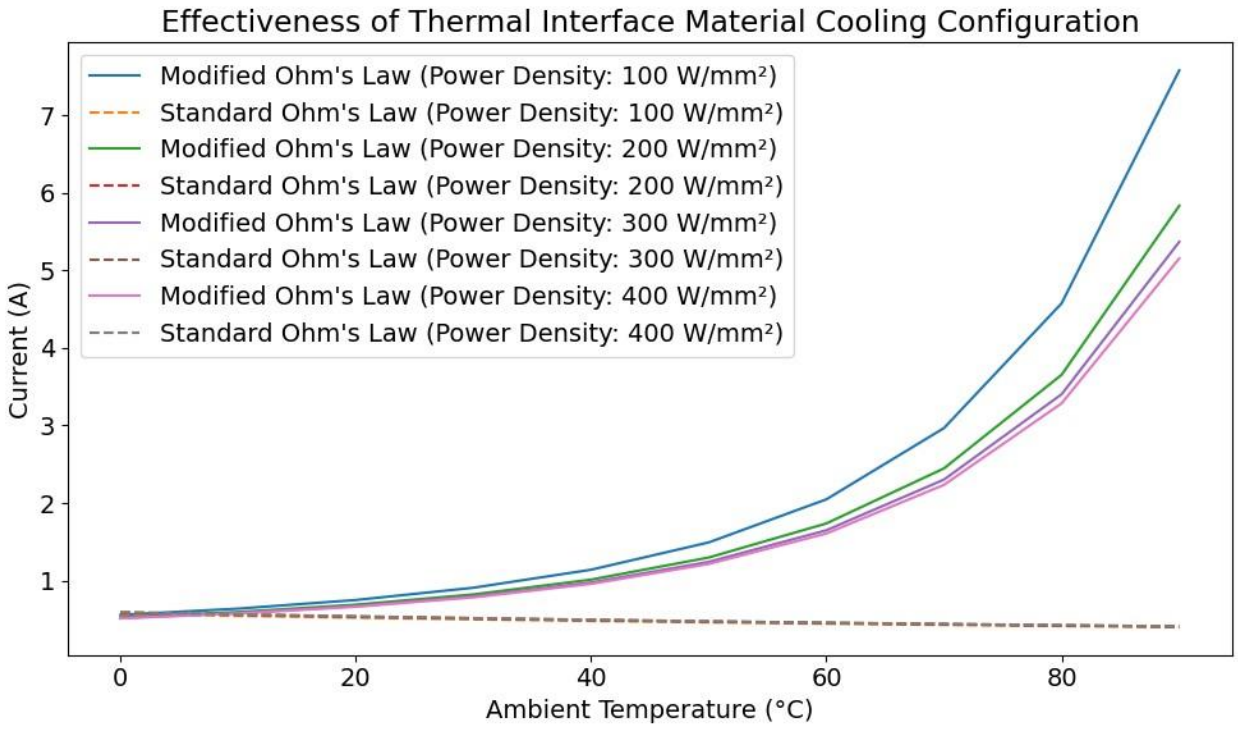


**Figure 7.** Thermal Interface Materials (TIMs) Impact on Heat Dissipation Effectiveness. (The figure shows that higher thermal conductivity TIMs result in smaller changes in current, indicating more effective heat dissipation, while lower thermal conductivity TIMs lead to larger current variations, reflecting higher thermal resistance and less efficient heat dissipation. The non-linear trends observed underscore the necessity of utilizing a Modified Ohm's Law framework for accurate modeling in scenarios influenced by varying TIM properties.)

**Validation Remark 4**. Through this analysis, it is evident that the Modified Ohm's Law offers a more suitable framework for accurately modeling the thermal behavior influenced by varying Thermal Interface Materials (TIMs) properties. The non-linear trends observed in the analysis, particularly in Figures 5,6 and 7, highlight the inadequacy of the Standard Ohm's Law, which assumes a linear relationship between current and voltage. In contrast, the Modified Ohm's Law, by incorporating temperature-dependent variations in resistance, better captures the complex interplay between thermal effects and electrical behavior, offering enhanced predictive capabilities in scenarios where TIM properties significantly impact heat dissipation

effectiveness. Therefore, for this specific application, the Modified Ohm's Law emerges as the preferred choice for modeling heat dissipation dynamics.

### 4.1.5 Validation and Comparative Analysis of Standard and Modified Ohm's Law Models

To validate the practical suitability of the Modified Ohm's Law against the Standard Ohm's Law, we conducted a thorough analysis using synthetic experimental simulation data generation and fitting both models on this dataset. This involved employing Finite Element Method (FEM) for computing temperature distributions, followed by calculating prediction error margins between the two models and the generated synthetic experimental data.

**Comparative Analysis of Standard and Modified Ohm's Law Predictions.** In this section, we examine the predictions of Standard and Modified Ohm's Law models in comparison with experimental data. Figure 8(a) portrays the prediction of Standard Ohm's Law (blue line) against the experimental data (green line), while Figure 8(b) illustrates the prediction of Modified Ohm's Law (red line) against the same experimental data. Analyzing both figures allows us to discern nuanced differences in how each model aligns with the experimental results. Both Standard and Modified Ohm's Law models appear to capture the overall trend of the experimental data, as indicated by the similarity in the shapes of the curves (green and blue/red lines) in both figures. This suggests that both models predict a comparable relationship between the independent variable (likely voltage or current) and the dependent variable (resistance or temperature). However, deviations from the experimental data are evident in both models. These discrepancies are particularly noticeable in regions where the experimental data exhibits sharp variations or steeper slopes. In Figure 8(a), the prediction of Standard Ohm's Law (blue line) demonstrates a slightly larger deviation from the experimental data (green line) compared to the Modified Ohm's Law in Figure 8(b). This disparity is especially apparent in regions with steeper slopes or sharp changes. The blue line appears smoother and less responsive to these rapid variations in the experimental data. Conversely, the prediction by Modified Ohm's Law (red line) in Figure 8(b) seems to better capture the sharp variations observed in the experimental data (green line). The red line more closely follows the steeper slopes and trends of the green line, indicating a stronger correlation between the model and the experimental observations. These discrepancies between the predictions and the experimental data may stem from the inherent limitations of each model. Standard Ohm's Law assumes a constant linear relationship between voltage and current, which might not hold true for real-world materials, especially at higher temperatures or voltage ranges. This non-linearity could explain why the Standard Ohm's Law prediction deviates more from the experimental data, particularly in regions with steeper slopes.

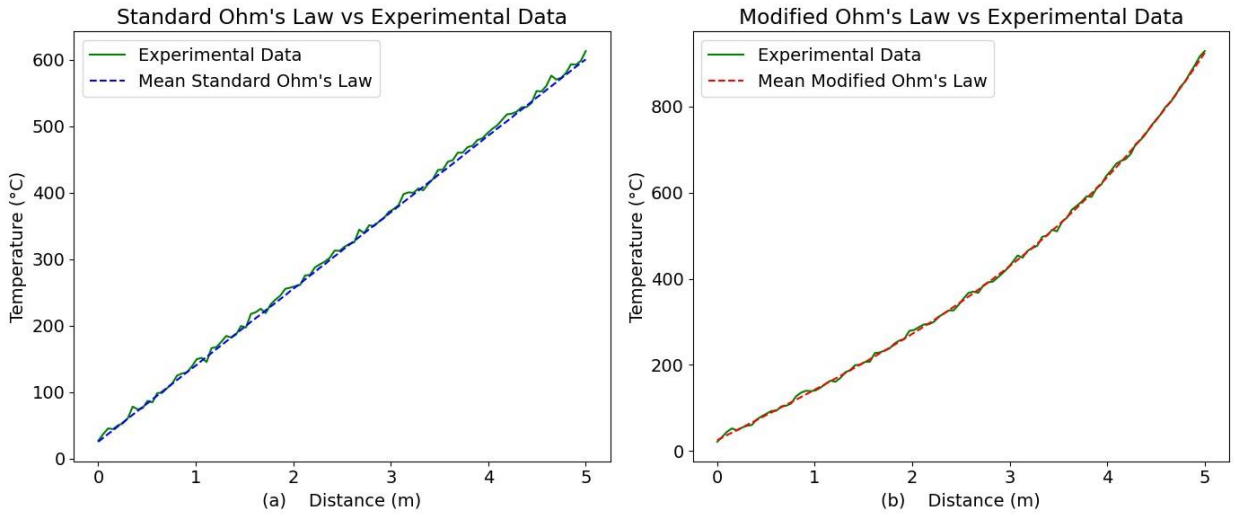


**Figure 8.** Comparison of model predictions with experimental data. (The blue line in Figure 8(a) represents the Standard Ohm's Law prediction, while the red line in Figure 8(b) shows the prediction from the Modified Ohm's Law. Both plots are overlaid with the experimental data represented by the green line. This allows for a direct comparison of the predicted temperature profiles with the actual measurements along the device (denoted by Distance (m)) and across the temperature range (indicated by Temperature (°C))).

On the other hand, Modified Ohm's Law incorporates the temperature dependence of resistance or other non-idealities, potentially providing a more accurate representation of the physical phenomena at play. This could elucidate why the Modified Ohm's Law prediction (red line) in Figure 8(b) demonstrates better alignment with the experimental data (green line), especially in areas with rapid changes. In the essence, the analysis of Figure 8(a) and Figure 8(b) suggests that both Standard and Modified Ohm's Law models can predict the general trend of the experimental data. However, Modified Ohm's Law appears to offer a more accurate representation, particularly in capturing the variations observed in the experimental results. This result highlights the importance of considering non-linear relationships and material properties when modeling real-world systems for improved accuracy.

**Error Distribution Analysis and Comparison of Standard and Modified Ohm's Laws.** The analysis is aimed at comparing the prediction accuracies of Standard and Modified Ohm's Laws in the context of temperature prediction based on simulated experimental data. In Figure 9, the distribution of prediction errors for both models is illustrated. Here, the horizontal axis represents the absolute error (°C), indicating the disparity between the predicted temperature values and the actual experimental temperatures. The vertical axis denotes the probability density, reflecting the likelihood of encountering specific error values. Upon examination of the error distributions depicted by the blue and red lines, insights into the prediction accuracies of each model emerge. The broader spread of the blue line associated with Standard Ohm's Law suggests a wider range of error values, indicating a higher probability of encountering larger deviations from the actual experimental temperatures. Conversely, the narrower distribution represented by the red line corresponding to Modified Ohm's Law implies that prediction errors are concentrated within a smaller range, suggesting a higher likelihood of predictions being closer to the actual temperatures. The observation of marginally smaller errors for Modified Ohm's Law aligns with the analysis of the error distributions. The reduced spread of errors, clustered closer to zero on the error index with device distance (m), indicates a higher degree of accuracy in temperature prediction compared to Standard Ohm's Law. This difference underscores the potential advantages of employing the Modified Ohm's Law over its standard counterpart in practical applications where precise temperature predictions are pivotal. The comparison drawn from Figure 9 suggests that Modified Ohm's Law offers slightly superior prediction accuracy compared to Standard Ohm's Law when applied to temperature prediction tasks based on simulated experimental data. While both models yield reasonable predictions, the narrower error distribution observed with Modified Ohm's Law signifies a closer alignment with the experimental data. This finding underscores the significance of utilizing more complex models, such as Modified Ohm's Law, to enhance temperature prediction accuracy, particularly in critical engineering applications where even minor temperature fluctuations can have substantial implications on performance and reliability.

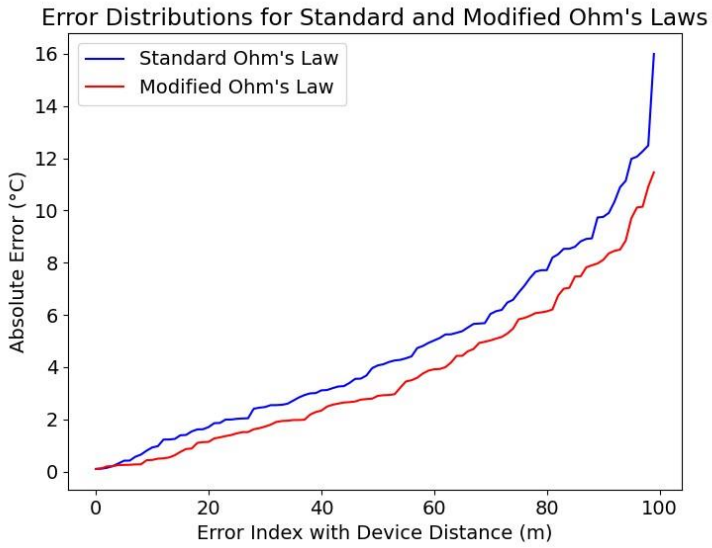


**Figure 9.** Error distributions for Standard and Modified Ohm's Law compared against synthetic experimental data. (These results illustrates the distribution of prediction errors for both Standard (blue line) and Modified (red line) Ohm's Laws compared against synthetic experimental data (likely temperature values). The horizontal axis represents the error index with device distance (m), which implies the spatial position within the thermal device where the errors occur. The vertical axis denotes the absolute error (°C), indicating the magnitude of deviation between the predicted and actual temperatures).

**Remark on Long Device Distances in Analysis (Scaling for Simulation).** The application of long device distances, such as 100 meters, within the analysis serves as a scaling factor within the simulation framework rather than representing physical dimensions of a semiconductor device. This abstraction allows for the exploration of temperature distributions and thermal behavior at a macroscopic level, enabling insights into system-level performance and thermal management strategies. While the distances utilized may appear large in the context of semiconductor devices, they facilitate comprehensive analysis and understanding of thermal phenomena across extended spatial domains within the simulation environment.

## 5. DİSCUSSİON

The results of simulated experiments provide compelling evidence for the effectiveness of the Modified Ohm's Law in addressing thermal management challenges in high-power semiconductor devices. This section delves into a detailed analysis, comparing it with the Standard Ohm's Law, to elucidate the strengths of the modified approach in thermal simulations. It also explores the significance of the validation process in understanding thermal behavior and its implications for optimizing cooling strategies.

### 5.1 Strengths of the Modified Ohm's Law in Thermal Simulations

The Modified Ohm's Law offers several advantages over the Standard Ohm's Law for simulating the intricate thermal dynamics of high-power semiconductor devices. A key strength lies in its ability to capture the non-linear relationships between temperature (T), current (I), and resistance (R). Unlike the Standard Ohm's Law, which assumes a linear proportionality ($I = V/R$), the modified version incorporates an exponential term to account for temperature-dependent variations in resistance $\left(I_{modified} = a \times e^{\frac{R_{short}}{R_0}}\right)$, [37]. This formulation aligns with the physics of semiconductor materials, where resistance increases with rising temperature due to lattice vibrations and carrier scattering [65,66]. This enhanced accuracy in predicting device temperature under varying operating conditions is crucial for optimizing cooling strategies and ensuring the reliability and longevity of semiconductor devices in real-world applications. Furthermore, the Modified Ohm's Law provides a more comprehensive framework for modeling heat dissipation mechanisms. By incorporating additional terms or equations that account for factors such as thermal conductivity $(k)$ and thermal resistance $(R_{th})$ in practice, the modified approach offers a more nuanced understanding of the thermal behavior of semiconductor devices.

### 5.2 Validation Process Strengthens Understanding of Thermal Behavior

The comparison of predictions from standard and Modified Ohm's Law models with experimental data serves a critical role. This process validates the accuracy of simulation techniques employed by engineers and exposes areas for improvement. In our study, this comparison revealed the Modified Ohm's Law's consistent advantage over the standard approach in predicting device temperature, especially in regions with rapid thermal variations. This validation not only bolsters confidence in the Modified Ohm's Law model but also offers valuable insights into the fundamental thermal dynamics of semiconductor devices. Beyond theoretical validation, the process facilitates the refinement of simulation parameters and model assumptions to better reflect real-world conditions. Key parameters in the Modified Ohm's Law, such as $R_{short}$ (representing variable resistance) and $a$ (current scaling factor), can be adjusted based on experimental data to improve the accuracy and reliability of thermal simulations. This iterative approach leads to more informed decision-making in device design and optimization. The reference resistance $(R_0)$ in the Modified Ohm's Law can also be calibrated to match the specific characteristics of the semiconductor device being modeled.

### 5.3 Implications for Optimizing Cooling Strategies

The Modified Ohm's Law's implications extend beyond theoretical modeling. It impacts practical applications by improving cooling strategies for high-power semiconductor devices. Analysis demonstrates that this modified approach offers superior accuracy and predictive capabilities compared to the Standard Ohm's Law, particularly in scenarios influenced by factors such as thermal interface materials (TIMs) and heat sink configurations. TIMs with varying thermal conductivities can significantly impact heat transfer efficiency between the device and the heat sink. The Modified Ohm's Law has demonstrated the ability to account for these variations by incorporating the thermal conductivity of the TIM into the model. Similarly, heat sink configurations with larger surface areas or improved airflow characteristics can enhance heat dissipation. The Modified Ohm's Law has shown the potential that it can be used to predict the effectiveness of different heat sink designs by incorporating their thermal resistance into the model. Thermal simulations based on Modified Ohm's Law provide engineers with valuable insights.

These insights can be used to optimize cooling strategies, mitigate thermal issues, and enhance device performance. For instance, simulations might identify configurations with larger heat sinks or more thermally conductive thermal interface materials (TIMs) that result in lower device temperatures. This information directly translates to the selection of appropriate cooling components, ensuring optimal device operation and preventing thermal runaway scenarios.

## 6. CONCLUSİON

Throughout the analysis, a modified version of Ohm's Law was applied to address the intricate thermal management challenges encountered in high-power semiconductor devices. Acknowledging the non-linear relationship between temperature, current, and resistance, the paper aimed to establish a more accurate and reliable method for modeling thermal behavior, ultimately enhancing cooling strategies and mitigating thermal issues. The workflow has demonstrated the effectiveness of the Modified Ohm's Law in addressing thermal management challenges inherent in high-power semiconductor devices. This paper presents one of the initial conventional applications of the Modified Ohm's Law within this domain, achieved through scrupulous combination of simulations and empirical validation. Integrating temperature-dependent variations in resistance, the modified approach offers a more refined representation of the complex thermal dynamics within these devices. This advancement not only deepens engineers' understanding but also enhances their predictive capability concerning semiconductor device behavior across various operating conditions, thereby facilitating the development of more effective thermal management strategies. A critical revelation of our analysis lies in the strengths exhibited by the Modified Ohm's Law when compared to the conventional approach. Firstly, the modified version adeptly captures the non-linear relationship between temperature, current, and resistance, resulting in more precise predictions of device temperature, particularly in scenarios characterized by rapid temperature fluctuations. Secondly, by incorporating factors such as thermal conductivity and thermal resistance, the Modified Ohm's Law provides a comprehensive framework for modeling heat dissipation mechanisms. This feature enables researchers and engineers to design cooling systems tailored to specific device configurations and operating environments, thereby enhancing overall efficiency. The validation process served as a cornerstone in solidifying our comprehension of thermal behavior within high-power semiconductor devices. Through rigorous comparisons between model predictions and simulated experimental data validated the modified approach's accuracy and yielded invaluable insights into the underlying thermal dynamics. This iterative process not only bolstered confidence in the Modified Ohm's Law model but also facilitated the refinement of simulation parameters and model assumptions. Consequently, this iterative refinement process enables more informed decision-making during device design and optimization endeavors. Beyond theoretical implications, the findings of this study bear practical significance in optimizing cooling strategies for high-power semiconductor devices. Leveraging insights gleaned from thermal simulations, engineers can identify optimal cooling configurations to mitigate thermal issues and enhance device performance. Notably, the analysis underscored that configurations featuring larger heat sinks or more thermally conductive interface materials tend to yield lower device temperatures. Such insights can guide the selection of appropriate cooling components to ensure optimal device operation and avert thermal-related malfunctions.

## SIMILARITY RATE: 5%

## AUTHOR CONTRIBUTION

First Author: Conceptualization, methodology, data curation, writing, editing etc.

## CONFLICT of INTEREST

The authors declared that they have no known conflict of interest.

## REFERENCES

[1] N. Hossain et al., "Advances and significances of nanoparticles in semiconductor applications – A review," Results Eng., vol. 19, p. 101347, Sep. 2023, doi: 10.1016/j.rineng.2023.101347.

[2] B. K. Bose, "Global Energy Scenario and Impact of Power Electronics in 21st Century," IEEE Trans. Ind. Electron., vol. 60, no. 7, pp. 2638–2651, Jul. 2013, doi: 10.1109/TIE.2012.2203771.

[3] R. Singh, S. V. Akram, A. Gehlot, D. Buddhi, N. Priyadarshi, and B. Twala, "Energy System 4.0: Digitalization of the Energy Sector with Inclination towards Sustainability," Sensors, vol. 22, no. 17, p. 6619, Sep. 2022, doi: 10.3390/s22176619.

[4] M. Kumar, K. P. Panda, R. T. Naayagi, R. Thakur, and G. Panda, "Comprehensive Review of Electric Vehicle Technology and Its Impacts: Detailed Investigation of Charging Infrastructure, Power Management, and Control Techniques," Appl. Sci., vol. 13, no. 15, Art. no. 15, Jan. 2023, doi: 10.3390/app13158919.

[5] M. Schulz, "Thermal management details and their influence on the aging of power semiconductors," in 2014 16th European Conference on Power Electronics and Applications, Lappeenranta, Finland: IEEE, Aug. 2014, pp. 1–6. doi: 10.1109/EPE.2014.6910898.

[6] T. Zhan et al., "Effects of Thermal Boundary Resistance on Thermal Management of Gallium-Nitride-Based Semiconductor Devices: A Review," Micromachines, vol. 14, no. 11, p. 2076, Nov. 2023, doi: 10.3390/mi14112076.

[7] Kim, Kwang-Seok, Choi, Don-Hyun, and Jung, Seung-Boo, "Overview on Thermal Management Technology for High Power Device Packaging," J. Microelectron. Packag. Soc., vol. 21, no. 2, pp. 13–21, Jun. 2014, doi: 10.6117/KMEPS.2014.21.2.013.

[8] Thermal and Power Management of Integrated Circuits. in Series on Integrated Circuits and Systems. Boston: Kluwer Academic Publishers, 2006. doi: 10.1007/0-387-29749-9.

[9] V. Bianco, M. De Rosa, and K. Vafai, "Phase-change materials for thermal management of electronic devices," Appl. Therm. Eng., vol. 214, p. 118839, Sep. 2022, doi: 10.1016/j.applthermaleng.2022.118839.

[10] S. Rafin, R. Ahmed, Md. Haque, Md. Hossain, Md. Haque, and O. Mohammed, "Power Electronics Revolutionized: A Comprehensive Analysis of Emerging Wide and Ultrawide Bandgap Devices," Micromachines, vol. 14, no. 11, p. 2045, Oct. 2023, doi: 10.3390/mi14112045.

[11] T. Van Do, J. P. F. Trovão, K. Li, and L. Boulon, "Wide-Bandgap Power Semiconductors for Electric Vehicle Systems: Challenges and Trends," IEEE Veh. Technol. Mag., vol. 16, no. 4, pp. 89–98, Dec. 2021, doi: 10.1109/MVT.2021.3112943.

[12] J. R. Celaya, P. Wysocki, V. Vashchenko, S. Saha, and K. Goebel, "Accelerated aging system for prognostics of power semiconductor devices," in 2010 IEEE AUTOTESTCON, Orlando, FL, USA: IEEE, Sep. 2010, pp. 1–6. doi: 10.1109/AUTEST.2010.5613564.

[13] J. Jaguemont and J. Van Mierlo, "A comprehensive review of future thermal management systems for battery-electrified vehicles," J. Energy Storage, vol. 31, p. 101551, Oct. 2020, doi: 10.1016/j.est.2020.101551.

[14] M. Uzair, G. Abbas, and S. Hosain, "Characteristics of Battery Management Systems of Electric Vehicles with Consideration of the Active and Passive Cell Balancing Process," World Electr. Veh. J., vol. 12, no. 3, p. 120, Aug. 2021, doi: 10.3390/wevj12030120.

[15] S. S. Madani, C. Ziebert, and M. Marzband, "Thermal Behavior Modeling of Lithium-Ion Batteries: A Comprehensive Review," Symmetry, vol. 15, no. 8, p. 1597, Aug. 2023, doi: 10.3390/sym15081597.

[16] K. Gorecki and J. Zarebski, "Nonlinear Compact Thermal Model of Power Semiconductor Devices," IEEE Trans. Compon. Packag. Technol., vol. 33, no. 3, pp. 643–647, Sep. 2010, doi: 10.1109/TCAPT.2010.2052052.

[17] A. M. Darwish, A. J. Bayba, A. Khorshid, A. Rajaie, and H. A. Hung, "Calculation of the Nonlinear Junction Temperature for Semiconductor Devices Using Linear Temperature Values," IEEE Trans. Electron Devices, vol. 59, no. 8, pp. 2123–2128, Aug. 2012, doi: 10.1109/TED.2012.2200040.

[18] M. Janicki, Z. Sarkany, and A. Napieralski, "Impact of nonlinearities on electronic device transient thermal responses," Microelectron. J., vol. 45, no. 12, pp. 1721–1725, Dec. 2014, doi: 10.1016/j.mejo.2014.04.043.

[19] O. Yamashita, "Effect of linear and non-linear components in the temperature dependences of thermoelectric properties on the energy conversion efficiency," Energy Convers. Manag., vol. 50, no. 8, pp. 1968–1975, Aug. 2009, doi: 10.1016/j.enconman.2009.04.019.

[20] J. L. Smoyer and P. M. Norris, "Brief Historical Perspective in Thermal Management and the Shift Toward Management at the Nanoscale," Heat Transf. Eng., vol. 40, no. 3–4, pp. 269–282, Feb. 2019, doi: 10.1080/01457632.2018.1426265.

[21] D. Bandhu, M. D. Khadir, A. Kaushik, S. Sharma, H. A. Ali, and A. Jain, "Innovative Approaches to Thermal Management in Next-Generation Electronics," E3S Web Conf., vol. 430, p. 01139, 2023, doi: 10.1051/e3sconf/202343001139.

[22] Z. He, Y. Yan, and Z. Zhang, "Thermal management and temperature uniformity enhancement of electronic devices by micro heat sinks: A review," Energy, vol. 216, p. 119223, Feb. 2021, doi: 10.1016/j.energy.2020.119223.

[23] N. A. Pambudi, A. Sarifudin, R. A. Firdaus, D. K. Ulfa, I. M. Gandidi, and R. Romadhon, "The immersion cooling technology: Current and future development in energy saving," Alex. Eng. J., vol. 61, no. 12, pp. 9509–9527, Dec. 2022, doi: 10.1016/j.aej.2022.02.059.

[24] M. Ekpu, R. Bhatti, N. Ekere, S. Mallik, E. Amalu, and K. Otiaba, "Investigation of effects of heat sinks on thermal performance of microelectronic package," in 3rd IEEE International Conference on Adaptive Science and Technology (ICAST 2011), Abuja, Nigeria: IEEE, Nov. 2011, pp. 127–132. doi: 10.1109/ICASTech.2011.6145164.

[25] M. C. Shaw et al., "Enhanced thermal management by direct water spray of high-voltage, high power devices in a three-phase, 18-hp AC motor drive demonstration," in ITherm 2002. Eighth Intersociety Conference on Thermal and

Thermomechanical Phenomena in Electronic Systems (Cat. No.02CH37258), San Diego, CA, USA: IEEE, 2002, pp. 1007–1014. doi: 10.1109/ITHERM.2002.1012567.

[26] L. He, H. Jing, Y. Zhang, P. Li, and Z. Gu, "Review of thermal management system for battery electric vehicle," J. Energy Storage, vol. 59, p. 106443, Mar. 2023, doi: 10.1016/j.est.2022.106443.

[27] R. S. Longchamps, X.-G. Yang, and C.-Y. Wang, "Fundamental Insights into Battery Thermal Management and Safety," ACS Energy Lett., vol. 7, no. 3, pp. 1103–1111, Mar. 2022, doi: 10.1021/acsenergylett.2c00077.

[28] W. Wang, X. Zhang, C. Xin, and Z. Rao, "An experimental study on thermal management of lithium ion battery packs using an improved passive method," Appl. Therm. Eng., vol. 134, pp. 163–170, Apr. 2018, doi: 10.1016/j.applthermaleng.2018.02.011.

[29] J. Cho and J. Woo, "Development and experimental study of an independent row-based cooling system for improving thermal performance of a data center," Appl. Therm. Eng., vol. 169, p. 114857, Mar. 2020, doi: 10.1016/j.applthermaleng.2019.114857.

[30] Xingsheng Liu, M. H. Hu, C. G. Caneau, R. Bhat, L. C. Hughes, and Chung-En Zah, "Thermal management strategies for high power semiconductor pump lasers," in The Ninth Intersociety Conference on Thermal and Thermomechanical Phenomena In Electronic Systems (IEEE Cat. No.04CH37543), Las Vegas, NV, USA: IEEE, 2004, pp. 493–500. doi: 10.1109/ITHERM.2004.1318324.

[31] L. Maguire, M. Behnia, and G. Morrison, "An Experimental and Computational Study of Heat Transfer in High Power Amplifiers," Heat Transf. Eng., vol. 26, no. 2, pp. 81–92, Mar. 2005, doi: 10.1080/01457630590897295.

[32] T. Zhang, "Analytical Solution of Nonlinear Thermoelectric Heat Transport Equation Using Homotopy Perturbation Method," J. Comput. Intell. Electron. Syst., vol. 4, no. 1, pp. 59–66, Mar. 2015, doi: 10.1166/jcies.2015.1115.

[33] Z. Hu, M. Cui, and X. Wu, "Real-Time Temperature Prediction of Power Devices Using an Improved Thermal Equivalent Circuit Model and Application in Power Electronics," Micromachines, vol. 15, no. 1, p. 63, Dec. 2023, doi: 10.3390/mi15010063.

[34] A. Ibrahim, M. Salem, M. Kamarol, M. Delgado, and M. K. Mat Desa, "Review of Active Thermal Control for Power Electronics: Potentials, Limitations, and Future Trends," IEEE Open J. Power Electron., vol. 5, pp. 414–435, Apr. 2024, doi: 10.1109/OJPEL.2024.3376086.

[35] M. Baumann, W. Wondrak, and J. Lutz, Insight into thermal management concepts for power electronics modules in automotive application. 2023.

[36] M. Sofwan, M. Z. Abdullah, and M. K. Abdullah, "Experimental study on the cooling performance of high power LED arrays under natural convection," IOP Conf. Ser. Mater. Sci. Eng., vol. 50, Dec. 2013, doi: 10.1088/1757-899X/50/1/012030.

[37] A. Kimuya, "THE MODIFIED OHM'S LAW AND ITS IMPLICATIONS FOR ELECTRICAL CIRCUIT ANALYSIS," Eurasian J. Sci. Eng. Technol., vol. 4, no. 2, pp. 59–70, Dec. 2023, doi: 10.55696/ejset.1373552.

[38] M. Thorsell, K. Andersson, M. Fagerlind, M. Sudow, P.-A. Nilsson, and N. Rorsman, "Thermal Study of the High-Frequency Noise in GaN HEMTs," IEEE Trans. Microw. Theory Tech., vol. 57, no. 1, pp. 19–26, Jan. 2009, doi: 10.1109/TMTT.2008.2009084.

[39] M. Tounsi, A. Oukaour, B. Tala-Ighil, H. Gualous, B. Boudart, and D. Aissani, "Characterization of high-voltage IGBT module degradations under PWM power cycling test at high ambient temperature," Microelectron. Reliab., vol. 50, no. 9–11, pp. 1810–1814, Sep. 2010, doi: 10.1016/j.microrel.2010.07.059.

[40] W.-H. Chi, T.-L. Chou, C.-N. Han, and K.-N. Chiang, "Analysis of Thermal Performance of High Power Light Emitting Diodes Package," in 2008 10th Electronics Packaging Technology Conference, Singapore, Singapore: IEEE, Dec. 2008, pp. 533–538. doi: 10.1109/EPTC.2008.4763488.

[41] Z. Zhang, X. Wang, and Y. Yan, "A review of the state-of-the-art in electronic cooling," E-Prime - Adv. Electr. Eng. Electron. Energy, vol. 1, p. 100009, 2021, doi: 10.1016/j.prime.2021.100009.

[42] S. Rashidi, N. Karimi, B. Sunden, K. C. Kim, A. G. Olabi, and O. Mahian, "Progress and challenges on the thermal management of electrochemical energy conversion and storage technologies: Fuel cells, electrolysers, and supercapacitors," Prog. Energy Combust. Sci., vol. 88, p. 100966, Jan. 2022, doi: 10.1016/j.pecs.2021.100966.

[43] B. Kumanek and D. Janas, "Thermal conductivity of carbon nanotube networks: a review," J. Mater. Sci., vol. 54, no. 10, pp. 7397–7427, May 2019, doi: 10.1007/s10853-019-03368-0.

[44] W. Yu, C. Liu, and S. Fan, "Advances of CNT-based systems in thermal management," Nano Res., vol. 14, no. 8, pp. 2471–2490, Aug. 2021, doi: 10.1007/s12274-020-3255-1.

[45] S. Huang et al., The effects of graphene-based films as heat spreaders for thermal management in electronic packaging. 2016, p. 892. doi: 10.1109/ICEPT.2016.7583272.

[46] P. Huang et al., "Graphene film for thermal management: A review," Nano Mater. Sci., vol. 3, Sep. 2020, doi: 10.1016/j.nanoms.2020.09.001.

[47] Q. Chen et al., "Recent advances in thermal-conductive insulating polymer composites with various fillers," Compos. Part Appl. Sci. Manuf., vol. 178, p. 107998, Mar. 2024, doi: 10.1016/j.compositesa.2023.107998.

[48] Y.-H. Zhao, Y.-F. Zhang, and S.-L. Bai, "High thermal conductivity of flexible polymer composites due to synergistic effect of multilayer graphene flakes and graphene foam," Compos. Part Appl. Sci. Manuf., vol. 85, pp. 148–155, Jun. 2016, doi: 10.1016/j.compositesa.2016.03.021.
[49] Z. Sun, J. W. Chew, N. J. Hills, K. N. Volkov, and C. J. Barnes, "Efficient FEA/CFD Thermal Coupling for Engineering Applications," in Volume 4: Heat Transfer, Parts A and B, Berlin, Germany: ASMEDC, Jan. 2008, pp. 1505–1515. doi: 10.1115/GT2008-50638.
[50] Z. Sun, J. W. Chew, N. J. Hills, K. N. Volkov, and C. J. Barnes, "Efficient Finite Element Analysis/Computational Fluid Dynamics Thermal Coupling for Engineering Applications," J. Turbomach., vol. 132, no. 3, p. 031016, Jul. 2010, doi: 10.1115/1.3147105.
[51] L. Yuan, S. Liu, M. Chen, and X. Luo, "Thermal Analysis of High Power LED Array Packaging with Microchannel Cooler," in 2006 7th International Conference on Electronic Packaging Technology, Shanghai, China: IEEE, Aug. 2006, pp. 1–5. doi: 10.1109/ICEPT.2006.359826.
[52] S. Kochupurackal Rajan, B. Ramakrishnan, H. Alissa, W. Kim, C. Belady, and M. Bakir, "Integrated Silicon Microfluidic Cooling of a High-Power Overclocked CPU for Efficient Thermal Management," IEEE Access, vol. 10, pp. 1–1, Jan. 2022, doi: 10.1109/ACCESS.2022.3179387.
[53] A. Usman, F. Xiong, W. Aftab, M. Qin, and R. Zou, "Emerging Solid-to-Solid Phase-Change Materials for Thermal-Energy Harvesting, Storage, and Utilization," Adv. Mater., vol. 34, no. 41, p. 2202457, Oct. 2022, doi: 10.1002/adma.202202457.
[54] K. Venkateswarlu and K. Ramakrishna, "Recent advances in phase change materials for thermal energy storage-a review," J. Braz. Soc. Mech. Sci. Eng., vol. 44, no. 1, p. 6, Jan. 2022, doi: 10.1007/s40430-021-03308-7.
[55] Z.-Q. Yu, M.-T. Li, and B.-Y. Cao, "A comprehensive review on microchannel heat sinks for electronics cooling," Int. J. Extreme Manuf., vol. 6, no. 2, p. 022005, Apr. 2024, doi: 10.1088/2631-7990/ad12d4.
[56] A. Bar-Cohen, J. J. Maurer, and A. Sivananthan, "Near-Junction Microfluidic Cooling for Wide Bandgap Devices," MRS Adv., vol. 1, no. 2, pp. 181–195, Jan. 2016, doi: 10.1557/adv.2016.120.
[57] M. I. Davidzon, "Newton's law of cooling and its interpretation," Int. J. Heat Mass Transf., vol. 55, no. 21–22, pp. 5397–5402, Oct. 2012, doi: 10.1016/j.ijheatmasstransfer.2012.03.035.
[58] H.-P. Hsu, T.-W. Tu, and J.-R. Chang, "An Analytic Solution for 2D Heat Conduction Problems with General Dirichlet Boundary Conditions," Axioms, vol. 12, no. 5, p. 416, Apr. 2023, doi: 10.3390/axioms12050416.
[59] G. Feltrin, "Dirichlet Boundary Conditions," in Positive Solutions to Indefinite Problems, in Frontiers in Mathematics. , Cham: Springer International Publishing, 2018, pp. 3–37. doi: 10.1007/978-3-319-94238-4_1.
[60] B. N. Biswas, S. Chatterjee, S. Mukherjee, and S. Pal, "A DISCUSSION ON EULER METHOD: A REVIEW," Electron. J. Math. Anal. Appl., vol. 1, pp. 294–317, Jun. 2013.
[61] J. Liu and Y. Hao, "Crank–Nicolson method for solving uncertain heat equation," Soft Comput., vol. 26, no. 3, pp. 937–945, Feb. 2022, doi: 10.1007/s00500-021-06565-9.
[62] E. Hairer and G. Wanner, "Stiff differential equations solved by Radau methods," J. Comput. Appl. Math., vol. 111, no. 1–2, pp. 93–111, Nov. 1999, doi: 10.1016/S0377-0427(99)00134-X.
[63] C. Milici, J. Tenreiro Machado, and G. Drăgănescu, "Application of the Euler and Runge–Kutta Generalized Methods for FDE and Symbolic Packages in the Analysis of Some Fractional Attractors," Int. J. Nonlinear Sci. Numer. Simul., vol. 21, no. 2, pp. 159–170, Apr. 2020, doi: 10.1515/ijnsns-2018-0248.
[64] R. Y. Rubinstein and D. P. Kroese, Simulation and the Monte Carlo Method, 1st ed. in Wiley Series in Probability and Statistics. Wiley, 2007. doi: 10.1002/9780470230381.
[65] M. A. Rahman, "A Review on Semiconductors Including Applications and Temperature Effects in Semiconductors," Am. Sci. Res. J. Eng. Technol. Sci., vol. 7, no. 1, Art. no. 1, Apr. 2014, Accessed: Mar. 29, 2024. [Online]. Available: https://asrjetsjournal.org/index.php/American_Scientific_Journal/article/view/693
[66] Y. Wu et al., "Lattice Strain Advances Thermoelectrics," Joule, vol. 3, no. 5, pp. 1276–1288, May 2019, doi: 10.1016/j.joule.2019.02.008.
[67] M. R. Hajmohammadi, M. Ahmadian, and S. S. Nourazar, "Introducing highly conductive materials into a fin for heat transfer enhancement," Int. J. Mech. Sci., vol. 150, pp. 420–426, Jan. 2019, doi: 10.1016/j.ijmecsci.2018.10.048.
[68] Á. Lakatos and A. Trník, "Thermal Diffusion in Fibrous Aerogel Blankets," Energies, vol. 13, no. 4, p. 823, Feb. 2020, doi: 10.3390/en13040823.

**Appendix I. Solver Implementation Framework**

Leveraging the Finite Element Method (FEM), the solver computes temperature distributions within the device under diverse operating conditions and cooling strategies. The solver integrates the one-dimensional heat conduction equation discretized using finite differences to solve for the temperature distribution over time. Boundary conditions, including ambient and hot temperatures, are applied to simulate heat transfer at device interfaces. Additionally, the solver incorporates parameters such as thermal diffusivity, spatial and temporal step sizes, and the length of the device to define the simulation domain and parameters. Through iteratively updating the temperature distribution at each spatial grid point using explicit Euler method, the solver effectively captures the thermal behavior of the semiconductor device.

**Python based Solver Implementation**

```
import numpy as np
import matplotlib.pyplot as plt

# Define parameters
L = 100.0  # Length of the device (m)
Nx = 100  # Number of spatial grid points
T_ambient = 25.0  # Ambient temperature (°C)
T_hot = 100.0  # Temperature of the hot end (°C)
alpha = 0.1  # Thermal diffusivity (m^2/s)
t_final = 100.0  # Final time for simulation (s)
dt = 0.01  # Time step size (s)
dx = L / Nx  # Spatial step size (m)

# Initialize temperature array
T = np.zeros(Nx)
T[0] = T_ambient
T[-1] = T_hot

# Perform time integration using explicit Euler method
for t in np.arange(0, t_final, dt):
    T_new = np.zeros(Nx)
    for i in range(1, Nx - 1):
        T_new[i] = T[i] + alpha * dt * (T[i+1] - 2*T[i] + T[i-1]) / dx**2
    T = T_new

# Plot temperature distribution
x = np.linspace(0, L, Nx)
plt.plot(x, T)
plt.xlabel('Distance (m)')
plt.ylabel('Temperature (°C)')
plt.title('Temperature Distribution')
plt.grid(True)
plt.show()

# Apply Ohm's Laws
# Standard Ohm's Law: V = RI
R_standard = 50.0  # Constant resistance value (Ω)
V_standard = R_standard * np.ones(Nx)  # Example voltage (V)

# Modified Ohm's Law: V_modified = a * e^(R_short / R_0 * x / L)
R_short = 400.0  # Short resistance (Ω)
R_0 = 100.0  # Reference resistance (Ω)
a = 1  # Constant for Modified Ohm's Law
x_values = np.linspace(0, L, Nx)
V_modified = a * np.exp(R_short / R_0 * x_values / L)
```

```
# Plot voltage distributions
plt.plot(x_values, V_standard, label='Standard Ohm\'s Law', color='blue')
plt.plot(x_values, V_modified, label='Modified Ohm\'s Law', color='red')
plt.xlabel('Distance (m)')
plt.ylabel('Voltage (V)')
plt.title('Voltage Distribution')
plt.grid(True)
plt.legend()
plt.show()
```

**Appendix II. Synthetic Data Generator**

A Monte Carlo simulation approach was utilized, enabling systematic exploration of a wide range of potential operating conditions by introducing perturbations within predefined ranges for material properties and boundary conditions. This variation, resembling real-world uncertainties, allowed for the random adjustment of parameters such as thermal conductivity and boundary temperatures for each sample within the simulation. Subsequently, temperature distributions were computed using the Finite Element Method (FEM), providing insight into the thermal behavior of the semiconductor device under diverse operating conditions and cooling strategies. To enhance the realism of the synthetic data, noise was incorporated into the temperature distributions, accounting for measurement errors and environmental uncertainties typically encountered in experimental scenarios.

**Python Based Synthetic Data Generator**

```
import numpy as np
import matplotlib.pyplot as plt
import pandas as pd

# Set font size
plt.rcParams.update({'font.size': 14})

# Define parameters
L = 5.0  # Length of the device (m)
Nx = 100  # Number of spatial grid points
T_ambient = 25.0  # Ambient temperature (°C)
T_hot = 100.0  # Temperature of the hot end (°C)
k_0 = 100  # Thermal conductivity at reference temperature (W/mK)
T_0 = 25.0  # Reference temperature (°C)
a = 1.0  # Constant for Modified Ohm's Law
R_0 = 100.0  # Reference resistance (Ω)
R_short = 50.0  # Short resistance (Ω)
noise_std = 5.0  # Standard deviation of noise

# Define spatial grid
x = np.linspace(0, L, Nx)

# Generate synthetic experimental data using Monte Carlo simulation
np.random.seed(0)  # for reproducibility
num_samples = 1000  # Number of Monte Carlo samples

# Initialize arrays to store synthetic data
temperature_standard_samples = np.zeros((num_samples, Nx))
temperature_modified_samples = np.zeros((num_samples, Nx))

# Finite Element Method (FEM) computation
for i in range(num_samples):
    # Perturb material properties or boundary conditions within some range
    k_material_perturbed = k_0 * np.exp(np.random.uniform(-0.1, 0.1, size=Nx))
    T_boundary_perturbed = np.linspace(np.random.uniform(20, 30), np.random.uniform(90, 110), Nx)

    # Calculate temperature distribution using Finite Element Method (FEM) for Standard Ohm's Law
    T_standard = np.zeros_like(x)
    for j in range(Nx):
        T_standard[j] = np.trapz(k_material_perturbed[:j + 1], x[:j + 1]) + T_boundary_perturbed[j]

    # Calculate temperature distribution using Finite Element Method (FEM) for Modified Ohm's Law
    T_modified = np.zeros_like(x)
    for j in range(Nx):
        T_modified[j] = np.trapz(
```

```
            k_material_perturbed[:j + 1] * np.exp(-a * R_short / R_0 * x[:j + 1] / L), x[:j + 1]) + T_boundary_perturbed[
                j]

    # Add noise to the temperature distributions
    temperature_standard_samples[i] = T_standard + np.random.normal(loc=0, scale=noise_std, size=Nx)
    temperature_modified_samples[i] = T_modified + np.random.normal(loc=0, scale=noise_std, size=Nx)

# Create DataFrame to store synthetic experimental data
df = pd.DataFrame({'Distance': x})
for i in range(num_samples):
    df[f'Temperature_Standard_{i}'] = temperature_standard_samples[i]
    df[f'Temperature_Modified_{i}'] = temperature_modified_samples[i]

# Save data to Excel
df.to_excel('synthetic_experimental_data.xlsx', index=False)
```

**Appendix III. Prediction Margins and Temperature Discrepancies**

The analysis also involved calculating the margins between the device temperatures predicted by standard and Modified Ohm's Laws, which are depicted in Figure 10. These margins represent the differences in temperature predictions between the two cooling strategies and offer valuable insights into the non-linear relationship between temperature and resistance.

**Non-linearity and Margin Variations.** A crucial observation from Figure 10 is that the margins between the temperature predictions are not constant across the entire range of ambient temperatures. The depicted results indicate that the margins vary as the ambient temperature increases from 0 °C to 80 °C. This variation contradicts the behavior expected from a strictly linear relationship between temperature and resistance, as assumed by the Standard Ohm's Law. In a scenario with a perfectly linear relationship, the difference in temperature predictions between the two Laws would be constant regardless of the ambient temperature. However, the observed variation in margins suggests a more complex interplay between temperature and resistance, which the Modified Ohm's Law aims to capture.

**Validation of Modified Ohm's Law.** The non-constant margins observed in Figure 10 validate the importance of considering the temperature dependence of resistance in thermal modeling. The Modified Ohm's Law incorporates this dependence through an exponential term or additional equations, allowing it to predict a more nuanced variation in temperature margins across different ambient conditions. While the Standard Ohm's Law might predict a constant difference in temperature throughout the operating range, the reality reflected in Figure 10 is likely to be closer to the non-linear behavior captured by the Modified Ohm's Law. This highlights the merit of the modified approach for accurate thermal simulations, particularly in scenarios where temperature variations are significant.

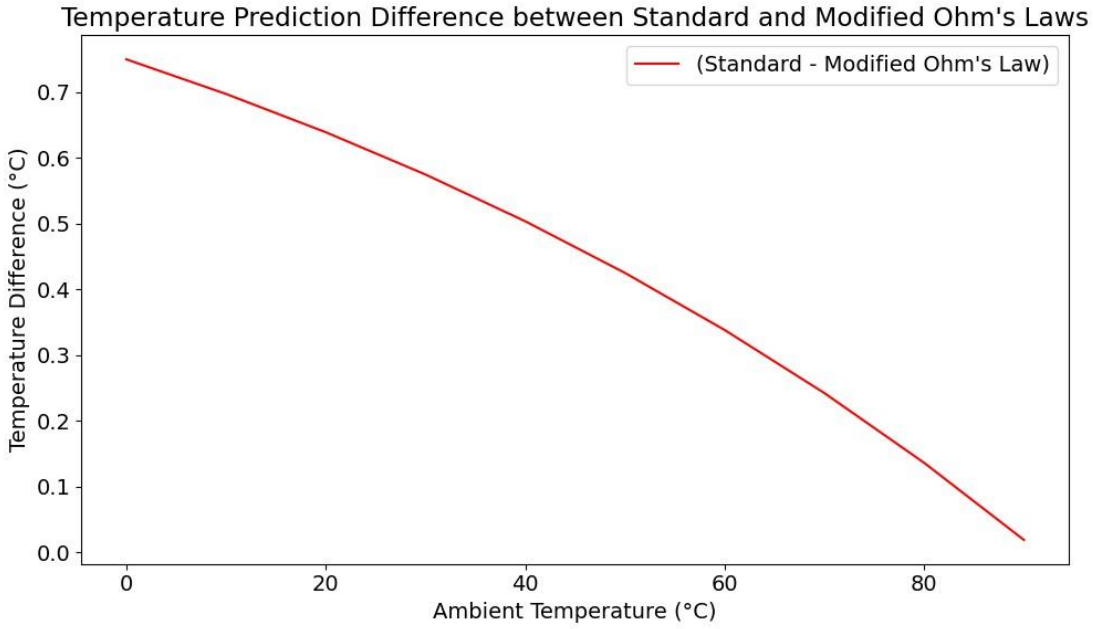


**Figure 10.** Temperature Prediction Margins between Standard and Modified Ohm's Laws.

**Appendix IV. Establishing a Simulation Framework**

This section outlines the development of a simulation framework to analyze heat generation and dissipation within a semiconductor device as worked out through section 3 and section 4.

**Geometric Parameters**

The chosen geometric parameters define the physical characteristics of the device and its surrounding environment, influencing thermal behavior.

**Device Geometry.** This section details the specifications for the device geometry, including the size and shape of the active regions, contact pads, and interconnects. These dimensions directly influence heat generation within the device.

**Substrate Properties.** The thickness and material properties of the underlying substrate play a critical role in heat conduction and dissipation. A substrate's thickness can significantly impact its thermal conductivity, with thicker substrates potentially exhibiting different thermal behavior compared to thinner ones.

**Heat Sink Design.** The design of the heat sink, responsible for transferring heat away from the device, will be scrupulously defined. Parameters including; fin dimensions, spacing, and orientation will be carefully considered to optimize heat transfer efficiency and maximize cooling performance.

**Material Properties**

Consideration is given to material properties, including thermal conductivity, specific heat capacity, and density, for various components within the semiconductor device, substrate, packaging, and cooling components. For this paper, we will choose the following material properties to represent the thermal characteristics of high-power semiconductor devices.

**Thermal Conductivity (κ).** This property signifies a material's ability to conduct heat. Materials with higher thermal conductivity can dissipate heat more efficiently, making them ideal for applications involving heat transfer [67].

**Specific Heat Capacity (cp).** Specific heat capacity refers to the amount of heat energy required to raise the temperature of one unit mass (typically 1 kilogram) of a material by one degree Celsius. This property influences a material's ability to store thermal energy.

**Density (ρ).** Density represents the mass per unit volume of a material. It plays a role in a material's thermal inertia, which is its resistance to temperature changes. Materials with higher density tend to have higher thermal inertia, meaning they require more heat energy to experience a significant temperature increase [68]. Additionally, density can influence a material's heat storage capacity, as denser materials can store more heat per unit volume.

**Boundary Conditions**

Choosing appropriate boundary conditions is essential for accurately modeling heat transfer at device interfaces. Boundary conditions govern heat fluxes, temperatures, and thermal resistances at junctions and interfaces, influencing the overall thermal performance of the device. The following boundary conditions to govern heat transfer at device interfaces are established.

**Heat Fluxes**. The rate of heat transfer per unit area at the device interfaces.

**Temperatures**. The initial temperatures assigned to different regions of the semiconductor device and the surrounding environment.

**Thermal Resistances**. The resistance to heat flow at junctions and interfaces between different materials.

These boundary conditions will be applied to govern heat transfer and temperature distribution within the simulated environment, allowing for a realistic representation of thermal behavior in high-power semiconductor devices.